Multi-scale analysis of fiber reinforced composite parts submitted to environmental and mechanical loads

Frédéric Jacquemin, Sylvain Fréour

Multi-scale analysis of fiber-reinforced composite parts submitted to environmental and mechanical loads

Jacquemin Frédéric, Fréour Sylvain

GeM -Institut de Recherche en Génie Civil et Mécanique

Université de Nantes-Ecole Centrale de Nantes-CNRS UMR 6183

37 Boulevard de l'Université, BP 406, 44 602 Saint-Nazaire, France

*Corresponding author: Fax number: +33240172618, **E-mail address:** sylvain.freour@univ-nantes.fr

Abstract

The purpose of this work is to present various application of statistical scale transition models to the analysis of polymer-matrix composites submitted to thermo-hygro-mechanical loads. In order to achieve such a goal, two approaches, classically used in the field of modelling heterogeneous material are studied: Eshelby-Kröner self-consistent model on the one hand and Mori-Tanaka approximate, on the second hand. Both models manage to handle the question of the homogenization of the microscopic properties of the constituents (matrix and reinforcements) in order to express the effective macroscopic coefficients of moisture expansion, coefficients of thermal expansion and elastic stiffness of a uni-directionally reinforced single ply. Inversion scale transition relations are provided also, in order to identify the effective unknown behaviour of a constituent. The proposed method entails to inverse scale transition models usually employed in order to predict the homogenised macroscopic elastic/hygroscopic/thermal properties of the composite ply from those of the constituents. The identification procedure involves the coupling of the inverse scale transition models to macroscopic input data obtained through either experiments or in the already published literature. Applications of the proposed approach to practical cases are provided: in particular, a very satisfactory agreement between the fitted elastic constants and the corresponding properties expected in practice for the reinforcing fiber of typical composite plies is achieved.
Another part of this work is devoted to the extensive analysis of macroscopic mechanical states concentration within the constituents of the plies of a composite structure submitted to thermo-hygro-elastic loads. Both numerical and a fully explicit version of Eshelby-Kröner model are detailed. The two approaches are applied in the viewpoint of predicting the mechanical states in both the fiber and the matrix of composites structures submitted to a transient hygro-elastic load. For this purpose, rigorous continuum mechanics formalisms are used for the determination of the required time and space dependent macroscopic stresses. The reliability of the new analytical approach is checked through a comparison between the local stress states calculated in both the resin and fiber according to the new closed form solutions and the equivalent numerical model: a very good agreement between the two models was obtained.
The purpose of the final part of this work consists in the determination of microscopic (local) quadratic failure criterion (in stress space) in the matrix of a composite structure submitted to purely mechanical load. The local failure criterion of the pure matrix is deduced from the macroscopic strength of the composite ply (available from experiments), using an appropriate inverse model involving the explicit scale transition relations previously obtained for the macroscopic stress concentration at microscopic level. Convenient analytical forms are

provided as often as possible, else procedures required to achieve numerical calculations are extensively explained. Applications of this model are achieved for two typical carbon-fiber reinforced epoxies: the previously unknown microscopic strength coefficients and ultimate strength of the considered epoxies are identified and compared to typical expected values published in the literature.

Keywords: scale transition modelling, homogenization, identification, polymer-matrix composites.

1- Introduction

Carbon-reinforced epoxy based composites offer design, processing, performance and cost advantages compared to metals for manufacturing structural parts. Among the advantages, provided by carbon-reinforced epoxies over metals and ceramics, that have been recognised for years, improved fracture toughness, impact resistance, strength to weight ratio as well as high resistance to corrosion and enhanced fatigue properties have often been put in good use for practical applications (Karakuzu et al., 2001).
Now, the accurate design and sizing of any structure requires the knowledge of the mechanical states experienced by the material for the possibly various loads, expected to occur during service life. Since high performance composites are being increasingly used in aerospace and marine structural applications, where they are exposed to severe environmental conditions, these composites experience hygrothermal loads as well as more classical mechanical loads. Now, unlike metallic or ceramic materials, composites are susceptible to both temperature *and* moisture when exposed to such working environments. These environmental conditions are known to possibly induce sometimes critical stresses distributions within the plies of the composite structures or even within their very constituents (i.e. the reinforcements on the one hand and the matrix on the second hand). Actually, carbon/epoxy composites can absorb significant amount of water and exhibit heterogeneous Coefficients of Moisture Expansion (CME) and Coefficients of Thermal Expansion (CTE) (i.e. the CME/CTE of the epoxy matrix are strongly different from the CME/CTE of the carbon fibers, as shown in: Tsai, 1987; Agbossou and Pastor, 1997; Soden et al., 1998), moreover, the diffusion of moisture in such materials is a rather slow process, resulting in the occurrence of moisture concentration gradients within their depth, during at least the transient stage (Crank, 1975). As a consequence, local stresses take place from hygro-thermal loading of composite structures which closely depends on the experienced environmental conditions, on the local intrinsic properties of the constituents and on its microstructure (the morphology of the constituents, the lay-up configuration, ... fall in this last category of factors). Now, the knowledge of internal stresses is necessary to predict a possible damage occurrence in the material during its manufacturing process or service life. Thus, the study of the development of internal stresses due to thermo-hygro-elastic loads in composites is very important in regard to any engineering application. Numerous papers, available in the literature, deal with this question, using Finite Element Analysis or Continuum Mechanics-based formalisms. These methods allow the calculation of the macroscopic stresses in each ply constituting the composite (Jacquemin and Vautrin, 2002). But, they do not provide information on the local mechanical states, in the fibers and matrix of a given ply, and, consequently, do not allow to explain the phenomenon of matrix cracking and damage development in composite structures, which originate at the microscopic level. The present work is precisely focused on the study of the internal stresses in the constituents of the ply. In order to reach this goal, scale transition models are required.

The present work underlines the potential of scale-transition models, as predictive tools, complementary to continuum mechanics in order to address: i) the estimation of the effective hygro-thermo-elastic properties of a composite ply from those of its constituents (section 2), ii) the identification of the hygro-thermo-elastic properties of one constituent of a composite ply (section 3), iii) the estimation of the local mechanical states experienced in each constituent of a composite structure (section 4), iv) the identification of the local strength of the constitutive matrix (section 5).
Section 6 of this paper is mainly dedicated to conclusions about the above listed sections the whereas section 7 is devoted to the introducing some scientifically appealing perspectives of research in the field of composites materials which are highly considered for further investigation in the forthcoming years.

2- Scale-transition model for predicting the macroscopic thermo-hygro-elastic properties of a composite ply

2-1- Introduction

Scale transition models are based on a multi-scale representation of materials. In the case of composite materials, for instance, a two-scale model is sufficient:

- The properties and mechanical states of either the resin or its reinforcements are respectively indicated by the superscripts ^{m} and ^{r}. These constituents define the so-called “pseudo-macroscopic” scale of the material (Sprauel and Castex, 1991).
- Homogenisation operations performed over its aforementioned constituents are assumed to provide the effective behaviour of the composite ply, which defines the macroscopic scale of the model. It is denoted by the superscript ^{I}. This definition also enables to consider an uni-directional reinforcement at macroscopic scale, which is a satisfactorily realistic statement, compared to the present design of composite structures (except for the particular case of woven-composites that will be specifically discussed in section 7.1).

As for the composite structure, it is actually constituted by an assembly of the above described composite plies, each of them possibly having the principal axis of their reinforcements differently oriented from one to another. This approach enables to treat the case of multi-directional laminates, as shown, for example, in (Fréour et al., 2005a).

2.2. The classical practical strategy for the direct application of homogenisation procedures

Within scale transition modeling, the local properties of the i–superscripted constituents are usually considered to be known (i.e. the pseudo-macroscopic stiffnesses, $\mathbf{L}^{i}$, coefficients of thermal expansion $\mathbf{M}^{i}$ and coefficients of moisture expansion $\boldsymbol{\beta}^{i}$), whereas the corresponding effective macroscopic properties of the composite structure (respectively, $\mathbf{L}^{I}$, $\mathbf{M}^{I}$ and $\boldsymbol{\beta}^{I}$) are a priori unknown and results from (often numerical) computations.
Among the numerous, available in the literature scale transition models, able to handle such a problem, most involve rough-and-ready theoretical frameworks: Voigt (Voigt, 1928), Reuss, (Reuss, 1929), Neerfeld-Hill (Neerfeld, 1942; Hill, 1952), Tsai-Hahn (Tsai and Hahn, 1980) and Mori-Tanaka (Mori and Tanaka, 1973; Tanaka and Mori, 1970) approximates fall in this category. This is not satisfying, since such a model does not properly depict the real physical conditions experienced in practice by the material. In spite of this lack of physical realism, some of the aforementioned models do nevertheless provide a numerically satisfying estimation of the effective properties of a composite ply, by comparison with the experimental

values or others, more rigorous models. Both Tsai-Hahn and Mori-Tanaka models fulfil this interesting condition (Jacquemin et al., 2005; Fréour et al., 2006a). Nevertheless, in the field of scale transition modelling, the best candidate remains Kröner-Eshelby self-consistent model, because only this model takes into account a rigorous treatment of the thermo-hygro-elastic interactions between the homogeneous macroscopic medium and its heterogeneous constituents, as well as this model enables handling the microstructure (i.e. the particular morphology of the constituents, especially that of the reinforcements).

2.3 Estimating the effective properties of a composite ply through Eshelby-Kröner self-consistent model

Self-consistent models based on the mathematical formalism proposed by Kröner (Kröner, 1958) constitute a reliable method to predict the micromechanical behavior of heterogeneous materials. The method was initially introduced to treat the case of polycrystalline materials, i.e. duplex steels, aluminium alloys, etc., submitted to purely elastic loads.
Estimations of homogenized elastic properties and related problems have been given in several works (François, 1991; Mabelly, 1996; Kocks et al., 1998). The model was thereafter extended to thermoelastic loads and gave satisfactory results on either single-phase (Turner and Tome, 1994; Gloaguen et al., 2002) or two-phases (Fréour et al., 2003a and 2003b) materials. More recently, this classical model was improved in order to take into account stresses and strains due to moisture in carbon fiber-reinforced polymer–matrix composites. Therefore, the formalism was extent so that homogenisation relations were established for estimating the macroscopic CME from those of the constituents (Jacquemin et al., 2005).

Many previously published documents have been dedicated to the determination of (at least some of) the effective thermo-hygro-elastic properties of heterogeneous materials through Kröner-Eshelby self-consistent approach (Kocks et al., 1998; Gloaguen et al., 2002; Fréour et al., 2003a-b; Jacquemin et al., 2005). The main involved equations are:

$$\mathbf{L^I} = \left\langle \mathbf{L^i} : \left(\mathbf{I} + \mathbf{E^I} : \left[\mathbf{L^i} - \mathbf{L^I} \right] \right)^{-1} \right\rangle_{i=r,m} \tag{1}$$

$$\boldsymbol{\beta}^{\mathbf{I}} = \frac{1}{\Delta C^{I}} \left\langle \left(\mathbf{L^i} + \mathbf{L^I} : \mathbf{R^I} \right)^{-1} : \mathbf{L^I} \right\rangle_{i=r,m}^{-1} : \left\langle \left(\mathbf{L^i} + \mathbf{L^I} : \mathbf{R^I} \right)^{-1} : \mathbf{L^i} : \boldsymbol{\beta}^{\mathbf{i}} \Delta C^{i} \right\rangle_{i=r,m} \tag{2}$$

$$\mathbf{M^I} = \left\langle \left[\mathbf{L^i} + \mathbf{L^I} : \mathbf{R^I} \right]^{-1} : \mathbf{L^I} \right\rangle_{i=r,m}^{-1} : \left\langle \left[\mathbf{L^i} + \mathbf{L^I} : \mathbf{R^I} \right]^{-1} : \mathbf{L^i} : \mathbf{M^i} \right\rangle_{i=r,m} \tag{3}$$

Where ΔC^i is the moisture content of the studied i element of the composite structure. The superscripts *r* and *m* are considered as replacement rule for the general superscript *i*, in the cases that the properties of the *reinforcements* or those of the *matrix* have to be considered, respectively. Actually, the pseudo-macroscopic moisture contents ΔC^r and ΔC^m can be expressed as a function of the macroscopic hygroscopic load ΔC^I (Loos and Springer, 1981), so that the hygro-mechanical states cancels in relation (2) that can finally be rewritten as a function of the materials properties only, but at the exclusion of the ΔC^i that are unexpected to appear in such an expression (Jacquemin et al., 2005). Relation (2), that is provided in the

present work for predicting the macroscopic CME, is given for its enhanced readability, compared to the more rigorous state exclusive relation.

In relations (1-3), the brackets < > stand for volume weighted averages (that in fact replace volume integrals that would require Finite Elements Methods instead). Empirically, as stated by Hill (Hill, 1952), arithmetic or geometric averages suggest themselves as good approximations. On the one hand, the geometric mean of a set of positive data is defined as the n^{th} root of the product of all the members of the set, where n is the number of members. On the other hand, in mathematics and statistics, the arithmetic mean (or simply the mean) of a list of numbers is the sum of all the members of the list divided by the number of items in the list. For Young's modulus, as an example, the Geometric Average Y^{GA} of the moduli according to the Reuss (Y_R) and Voigt (Y_V) models is defined as $Y^{GA} = \sqrt{Y_R\ Y_V}$, whereas the corresponding Arithmetic Average Y^{AA} is: $Y^{AA} = \frac{Y_R + Y_V}{2}$.

In statistics, given a set of data, X = { x_1, x_2, ..., x_n} and corresponding weights, W = { w_1, w_2, ..., w_n}, the weighted geometric (respectively, arithmetic) mean $\left\langle X^i \right\rangle^{GA}_{i=1,2,..., n}$ (respectively, $\left\langle X^i \right\rangle^{AA}_{i=1,2,..., n}$) is calculated as:

$$\left\langle X^i \right\rangle^{GA}_{i=1,2,..., n} = \left(\prod_{i=1}^{n} x_i^{w_i} \right)^{1/\left(\sum_{i=1}^{n} w_i \right)} \tag{4}$$

$$\left\langle X^i \right\rangle^{AA}_{i=1,2,..., n} = \frac{1}{\sum_{i=1}^{n} w_i} \sum_{i=1}^{n} x_i\ w_i \tag{5}$$

Both averages have been extensively used in the field of materials science, in order to achieve various scale transition modelling over a wide range of materials. The interested reader can refer to: (Morawiec, 1989; Matthies and Humbert, 1993; Matthies et al., 1994) that can be considered as typical illustrations of works taking advantage of the geometric average for estimating the properties and mechanical states of polycrystals (nevertheless, Eshelby-Kröner self-consistent model was not involved in any of these articles), whereas the previously cited references (Kocks et al., 1998; Gloaguen et al., 2002; Fréour et al., 2003; Jacquemin et al., 2005) show applications of arithmetic averages for studying of polycrystals or composite structures.

According to equations (4) and (5), the explicit writing of a volume weighted average directly depend on the averaging method chosen to perform this operation. Since the present work aims to express analytical forms involving such volume averages, it is necessary to select one average type in order to ensure a better understanding for the reader. Usually, in this field of research, the arithmetic and not the geometric volume weighted average is used. Moreover, in a recent work, the alternative geometric averages were also used for estimating the effective properties of carbon-epoxy composites (Fréour et al., to be published). Nevertheless, the obtained results were not found as satisfactory than in the previously studied cases of metallic

polycrystals or metal ceramic assemblies. Actually, the very strongly heterogeneous properties presented by the constituents of carbon reinforced polymer matrix composites yields a strong underestimation of the effective properties of the composite ply predicted according to Eshelby-Kröner model involving the geometric average, by comparison to the expected (measured) properties. Thus, the geometric average should not be considered as a reliable alternate solution to the classical arithmetic average for achieving scale transition modelling of composite structures. Consequently, arithmetic averages satisfying to relation (4) only will be used in the following of this manuscript.

Now, in the present case, where the macroscopic behaviour is described by two separate heterogeneous inclusions only (i.e. one for the matrix and one for the reinforcements), convenient simplifications of equation (5) do occur.
Actually, introducing v^r and v^m as the volume fractions of the ply constituents, and taking into account the classical relation on the summation over the volume fractions (i.e. $v^r + v^m = 1$), equation (5) applied to the volume average of any tensor A writes:

$$\left\langle \mathbf{A^i} \right\rangle_{i=r,m}^{AA} = \left\langle \mathbf{A^i} \right\rangle_{i=r,m} = v^r \, \mathbf{A^r} + v^m \, \mathbf{A^m} \tag{6}$$

In the following of the present work, the superscript AA denoting the selected volume average type will be omitted.

According to equations (1-3), the effective properties expressed within Eshelby-Kröner self-consistent model involve a still undefined tensor, $\mathbf{R^I}$. This term is the so-called "reaction tensor" (Kocks et al., 1998). It satisfies:

$$\mathbf{R^I} = \left(\mathbf{I} - \mathbf{S^I_{esh}}\right) : \mathbf{S^I_{esh}}^{-1} = \left(\mathbf{L^I}^{-1} - \mathbf{E^I}\right) : \mathbf{E^I}^{-1} \tag{7}$$

In the very preceding equation, $\mathbf{I}$ stands for the fourth order identity tensor. Hill's tensor $\mathbf{E^I}$, also known as Morris tensor (Morris, 1970), expresses the dependence of the reaction tensor on the morphology assumed for the matrix and its reinforcements (Hill, 1965). It can be expressed as a function of Eshelby's tensor $\mathbf{S^I_{esh}}$, through $\mathbf{E^I} = \mathbf{S^I_{esh}} : \mathbf{L^I}^{-1}$. It has to be underlined that both Hill's and Eshelby's tensor components are functions of the macroscopic stiffness $\mathbf{L^I}$ (some examples are given in Kocks et al., 1998; Mura, 1982).

In the case, when ellipsoidal-shaped inclusions have to be taken into account, the following general form enables the calculation of the components of this tensor (see the works of Asaro and Barnett, 1975 or Kocks et al. 1998):

$$\begin{cases} E^I_{ijkl} = \dfrac{1}{4\pi} \displaystyle\int_0^{\pi} \sin\theta \, d\theta \int_0^{2\pi} \gamma_{ikjl} \, d\varphi \\ \gamma_{ikjl} = \left[K^I_{ik}(\xi) \right]^{-1} \xi_j \, \xi_l \end{cases} \tag{8}$$

In the case of an orthotropic macroscopic symmetry, the components $K_{jp}(\xi)$ were given in (Kröner, 1953):

$$\mathbf{K^I} = \begin{bmatrix} L^I_{11}\xi_1^2 + L^I_{66}\xi_2^2 + L^I_{55}\xi_3^2 & \left(L^I_{12} + L^I_{66}\right)\xi_1\xi_2 & \left(L^I_{13} + L^I_{55}\right)\xi_1\xi_2 \\ \left(L^I_{12} + L^I_{66}\right)\xi_1\xi_2 & L^I_{66}\xi_1^2 + L^I_{22}\xi_2^2 + L^I_{44}\xi_3^2 & \left(L^I_{23} + L^I_{44}\right)\xi_2\xi_3 \\ \left(L^I_{13} + L^I_{55}\right)\xi_1\xi_2 & \left(L^I_{23} + L^I_{44}\right)\xi_2\xi_3 & L^I_{55}\xi_1^2 + L^I_{44}\xi_2^2 + L^I_{33}\xi_3^2 \end{bmatrix} \quad (9)$$

with

$$\xi_1 = \frac{\sin\theta\cos\varphi}{a_1}, \xi_2 = \frac{\sin\theta\sin\varphi}{a_2}, \xi_3 = \frac{\cos\theta}{a_3} \quad (10)$$

where 2 a_1, 2 a_2, 2 a_3 are the lengths of the principal axes of the ellipsoid (representing the considered inclusion) assumed to be respectively parallel to the longitudinal, transverse and normal directions of the sample reference frame.

According to equations (2-3, 7), the determination of both the macroscopic coefficients of thermal and moisture expansion are somewhat straightforward, while the effective stiffness is known, because the involved expressions are explicit. On the contrary, the estimation of the macroscopic stiffness of the composite ply through (1) cannot be as easily handled. Expression (1) is implicit because it involves $\mathbf{L^I}$ tensor in both its right and left members. Moreover, calculating the right member of equation (1) entails evaluating the reaction tensor (7) which also depends on the researched elastic stiffness, at least because of the occurrence of Hill's tensor (or Eshelby's tensor, if that notation is preferred) in relation (1). As a consequence, the effective elastic properties of a composite ply satisfying to Eshelby-Kröner self-consistent model constitutive relations are estimated at the end of an iterative numerical procedure. This is the main drawback of the self-consistent procedure preventing from achieving an analytical determination of the effective macroscopic thermo-hygro-elastic properties of a composite ply, in the case where this scale transition model is employed. Therefore, managing to express explicit solutions for estimating the macroscopic properties (or at least the macroscopic stiffness) requires focusing on a less intricate, less rigorous model but still providing realistic numerical values. Mori-Tanaka approach suggest itself as an appropriate candidate, for reasons that will be comprehensively explained in the next subsection.

2.4 Introducing Mori-Tanaka model as a possible alternate solution to Eshelby-Kröner model

As Eshelby-Kröner self-consistent approach, Mori Tanaka estimate is a scale transition model derived from the pioneering mathematical work of Eshelby (Eshelby, 1957). Mori and Tanaka actually investigated the opportunity of extending Eshelby's single-inclusion model (which is sometimes presented as an "infinitely dilute solution model") to the case where the volume fraction of the ellipsoidal heterogeneous inclusion embedded in the matrix is not tending towards zero anymore, but admits a finite numerical value (Mori and Tanaka, 1973; Tanaka and Mori, 1970). Calculations show that, in many cases, the effective homogenised macroscopic properties deduced from Mori-Tanaka approximate are close to their counterparts, estimated from the previously described Eshelby-Kröner self-consistent procedure (Baptiste, 1996, Fréour et al., 2006a). Exceptions to this statement occur nevertheless in the cases where extreme heterogeneities in the constituents properties have to be accounted for. For example, handling a significant porosities volume fraction yields Mori-Tanaka estimations deviating considerably from the self-consistent corresponding

calculations, according to (Benveniste, 1987). However, Mori-Tanaka approach is reported to remain reliable for treating cases similar to those aimed by the present work.

It has previously been demonstrated that the effective macroscopic homogenised thermo-hygro-elastic properties exhibited by a composite ply, according to Mori and Tanaka approximation satisfy the following relations (Baptiste, 1996; Fréour et al., 2006a):

$$\mathbf{L^I} = \left\langle \mathbf{T^i} : \left\langle \mathbf{L^i} : \mathbf{T^i} \right\rangle_{i=r,m}^{-1} \right\rangle_{i=r,m}^{-1} = \left\langle \mathbf{L^i} : \mathbf{T^i} \right\rangle_{i=r,m} : \left\langle \mathbf{T^i} \right\rangle_{i=r,m}^{-1} \tag{11}$$

$$\boldsymbol{\beta}^{\mathbf{I}} = \frac{1}{\Delta C^{I}} \left\langle \left(\mathbf{T^i} : \mathbf{L^i} : \left\langle \mathbf{L^i} : \mathbf{T^i} \right\rangle_{i=r,m}^{-1} \right)^{T} : \boldsymbol{\beta}^{\mathbf{i}} \Delta C^{i} \right\rangle_{i=r,m} \tag{12}$$

$$\mathbf{M^I} = \left\langle \left(\mathbf{T^i} : \mathbf{L^i} : \left\langle \mathbf{L^i} : \mathbf{T^i} \right\rangle_{i=r,m}^{-1} \right)^{T} : \mathbf{M^i} \right\rangle_{i=r,m} \tag{13}$$

The superscript ^{T} appearing in relations (12-13) denotes transposition operation.
The same remarks as indicated in the preceding subsection holds for the determination of the effective macroscopic CME using relation (12). This equation can be rewritten as a function of the materials properties only, thus excluding the moisture contents.

In equations (11-13), $\mathbf{T^i}$ is the elastic strain localisation tensor, expressed for the i-superscripted phase that is considered to interact with the embedding phase (denoted by the superscript e). Actually, Mori-Tanaka model is based on a two-step scale-transition procedure. In this theory, contrary to the case of Eshelby-Kröner self-consistent model, the inclusions are not considered to be directly embedded in the effective material having the behaviour of the composite structure (and thus interacting with it). In Mori and Tanaka approximation, the n constituents of a n-phase composite ply are separated in two subclasses: one of them is designed as the embedding constituent, whereas the n-1 others are considered as inclusions of the first one. The inclusion particles are embedded in the matrix phase, itself being loaded at the infinite by the hygro-mechanical conditions applied on the composite structure. In consequence, the inclusion phase does not experience any interaction with the macroscopic scale, but with the matrix only. In consequence, Mori and Tanaka model corresponds to the direct extension of Eshelby's single inclusion model (Eshelby, 1957) to the case that the volume fraction of inclusions does not remain infinitesimal anymore. Within Mori and Tanaka approach, this localisation tensor $\mathbf{T^i}$ writes as follows:

$$\mathbf{T^i} = \left[\mathbf{I} + \mathbf{E^i} : \left(\mathbf{L^i} - \mathbf{L^e} \right) \right]^{-1} \tag{14}$$

Contrary to the case of Eshelby-Kröner scale-transition model (refer to subsection 2.3. above), the localisation involved within Mori-Tanaka approximate does not explicitly involve the macroscopic stiffness. Nevertheless, according to the already cited same subsection, the reaction tensor involved in Eshelby-Kröner model was also implicitely depending on the macroscopic stiffness through the calculation procedure entailed for estimating Hill's tensor.

Within Mori-Tanaka procedure (Benveniste, 1987; Baptiste 1996; Fréour et al., 2006a), Hill's tensor $\mathbf{E^i}$ expresses the dependence of the strain localization tensor on the morphology assumed for the embedding phase and the particulates it surrounds (Hill, 1965). It can be expressed as a function of Eshelby's tensor $\mathbf{S^i_{esh}}$, through:

$$\mathbf{E^i} = \mathbf{S^i_{esh}} : \mathbf{L^{e^{-1}}} \tag{15}$$

In practice, the calculation of Hill's tensor for the embedded inclusions phase only would be necessary, since obvious simplifications of (14), leading to $\mathbf{T^e} = \mathbf{I}$, occur in the case that the embedding constituent localisation tensor is considered. According to relations (14-15), the strain localization tensor $\mathbf{T^i}$ does not involve the macroscopic stiffness tensor (or any other macroscopic property). As a consequence, contrary to Eshelby-Kröner self-consistent procedure, Mori-Tanaka approximation provides explicit relations (actually, the homogenization equations (11-13)) for estimating the researched macroscopic effective properties of a composite ply.

2.5 Example of homogenization : the case of T300-N5208 composites

The present subsection is focused on the application of the theoretical frameworks described in the above 2.3 and 2.4 sections to the numerical simulation of the effective properties of a typical, high-strength, fiber-reinforced composite made up of T300 carbon fibers and N5208 epoxy resin. The choice of such a material is justified because of the strong heterogeneities of the hygro-thermo-elastic properties of its constituents (actually, the numerical deviation occurring among the macroscopic properties of composites determined through various scale transition relations rises with this factor, see Jacquemin et al, 2005; Herakovich, 1998). Table 1 accounts for the pseudo-macroscopic properties reported in the literature for these constituents. The comparison between the results obtained through the two, considered in the present work alternate scale transition framework of Mori-Tanaka model are displayed on figure 1, for:

- the longitudinal and transverse Young's moduli Y^I_{11}, Y^I_{22},
- Coulomb's moduli G^I_{12}, G^I_{23},
- the coefficients of thermal expansion M^I_{11}, M^I_{22}
- the coefficients of moisture expansion β^I_{11}, β^I_{22}.

The calculations were achieved assuming that the reinforcements exhibit fiber-like morphology with an infinite length axis parallel to the longitudinal direction of the ply. For the determination of the CME, a perfect adhesion between the carbon fibers and the resin was assumed. Moreover, it also was assumed that the fibers do not absorb any moisture. Thus, the ratio between the pseudo-macroscopic and the macroscopic moisture contents is deduced from the expression given in (Loos and Springer, 1981):

$$\frac{\Delta C^m}{\Delta C^I} = \frac{\rho^I}{v^m \rho^m} \tag{16}$$

where ρ stands for the densities. The macroscopic density can be deduced form the classical rule of mixture:

$$\rho^I = v^m \rho^m + v^r \rho^r \quad (17)$$

The equations required for achieving Mori-Tanaka estimations involve relations (8-17). For the purpose of the strain localization, the embedding constituent was considered to be the epoxy matrix, whatever the considered volume fraction of reinforcements (thus, the transformation rule $\mathbf{L^e} = \mathbf{L^m}$ was considered to be valid in any case). Figure 1 also reports the numerical results obtained through Kröner-Eshelby Self-Consistent model (1-3, 6-10, 16-17), in the same conditions (identical inclusion morphology and constituents properties as for Mori-Tanaka computations).
Figure 1 shows the following interesting results:

- 1) In pure elasticity, both the investigated scale transition methods manage to reproduce the expected mechanical behaviour of the composite ply: the material is stiffer in the longitudinal direction than in the transverse direction. Moreover, the bounds are satisfying: the properties of the single constituents are correctly obtained for those of the composite ply in the cases where the epoxy volume fraction is either taken equal to v^m=0 (transversely isotropic elastic properties of T300 fibers) or v^m=1 (isotropic elastic properties of N5208 resin).
- 2) The curves drawn for each checked elastic constant are almost superposed, except for Coulomb's modulus G_{12}^I. Thus Mori-Tanaka model constitutes a rather reliable alternate homogenization procedure to Eshelby-Kröner rigorous solution for estimating the macroscopic elastic properties of typical carbon-epoxies.
- 3) Kröner-Eshelby self-consistent model and Mori-Tanaka approach both also do manage to achieve a realistic prediction of the macroscopic coefficients of thermal expansion. Especially, the expected boundary values are attained when the conditions v^m=1 (isotropic CTE of N5208 resin) or v^m=0 (transversely isotropic thermal properties of T300 fibers) are taken into account.
- 4) Mori-Tanaka approximate correctly reproduces the expected macroscopic coefficients of moisture expansion in the longitudinal direction. In the transverse direction, however, Mori-Tanaka model properly follows Eshelby Kröner model estimates while the epoxy volume fraction is higher than 0.5. In the range $0 \le v^m \le 0.5$, discrepancies occur between two considered scale transition models. In the case that the considered strain localization assumes the epoxy as the embedding constituent within Mori-Tanaka approximate, the relative error on β_{22}^I induced by this localization procedure, compared to Kröner-Eshelby reference values remains weaker than 9%, and falls below 6% in the range of epoxy volume fraction that is typical for designing composites structures for engineering applications $(0.3 \le v^m \le 0.7)$.
- 5) In the range of the epoxy volume fraction, that is typical for designing composites structures for engineering applications $\left(\text{i.e. } 0.3 \le v^m \le 0.7\right)$, according to the above discussed results 3) and 4), Mori-Tanaka model can be employed as an alternative to Eshelby-Kröner self-consistent model for estimating the effective macroscopic hygro-thermo-mechanical properties of composite plies.

The above listed elements 1) to 5) finally indicate that the effective macroscopic thermo-hygro-elastic properties of composite plies can be estimated in a reliable fashion using Mori-Tanaka approximate, assuming the epoxy as the embedding constituent, instead of the more

rigorous Kröner-Eshelby model. This statement is true while the epoxy volume fraction remains higher than 40%. Beyond this boundary value, some significant relative error (less than 10%) may be expected to occur in the estimated transverse CME.
The results, obtained in the present section, will be used in the following as input parameters for estimating the mechanical states experienced at macroscopic but at microscopic scale also in composite structures submitted to various loads (the interested reader should refer to section 4 for details).

3- Inverse scale transition modelling for the identification of the hygro-thermo-elastic properties of one constituent of a composite ply

3.1 Introduction

The precise knowledge of the pseudo-macroscopic properties of each constituent of a composite structure is required in order to achieve the prediction of its behavior (and especially its mechanical states) through scale transition models. Nevertheless, the pseudo-macroscopic stiffness, coefficients of thermal expansion and moisture expansion of the matrix and its reinforcements are not always fully available in the already published literature. The practical determination of the hygro-thermo-mechanical properties of composite materials are most of the time achieved on unidirectionnaly reinforced composites and unreinforced matrices (Bowles et al., 1981; Dyer et al., 1992; Ferreira et al., 2006a; Ferreira et al., 2006b; Herakovich, 1998; Sims et al., 1977). In spite of the existence of several articles dedicated to the characterization of the properties of the isolated reinforcements (Tsai and Daniel, 1994; DiCarlo, 1986; Tsai and Chiang, 2000), the practical achieving of this task remains difficult to handle, and the available published data for typical reinforcing particulates employed in composite design are still very limited. As a consequence, the properties of the single reinforcements exhibiting extreme morphologies (such as fibers), are not often known from direct experiment, but more usually they are deduced from the knowledge of the properties of the pure matrices and those of the composite ply (which both are easier to determine), through appropriate calculation procedures. The question of determining the properties of some constituents of heterogeneous materials has been extensively addressed in the field of materials science, especially for studying complex polycrystalline metallic alloys (like titanium alloys, cf. Fréour et al., 2002 ; 2005b ; 2006b) or metal matrix composites (typically Aluminum-Silicon Carbide composites cf. Fréour et al., 2003a ; 2003b or iron oxides from the inner core of the Earth, cf. Matthies et al., 2001, for instance). The required calculation methods involved in order to achieve such a goal are either based on Finite Element Analysis (Han et al., 1995) or on the inversion of scale transition homogenization procedures similar to those already presented in section 2 of the present paper. It was shown in previous works that it was actually possible to identify the properties of one constituent of a heterogeneous material from available (measured) macroscopic quantities through inverse scale transition models. Such identification methods were successfully used in the field of metal-matrix composites for the determination of the average elastic (Freour et al., 2002) and thermal (Freour et al., 2006b) properties of the β-phase of (α+β) titanium alloys. The procedure was recently extended to the study of the anisotropic elastic properties of the single-crystal of the β-phase of (α+β) titanium alloys on the basis of the interpretation of X-Ray Diffraction strain measurements performed on heterogeneous polycrystalline samples in (Freour et al., 2005b). The question of determining the temperature dependent coefficients of thermal expansion of silicon carbide was handled using a similar approach from measurements performed on aluminum – silicon carbide metal matrix composites in (Freour et al., 2003a; Freour et al.,

2003b).Numerical inversion of both Mori-Tanaka and Eshelby-Kröner self-consistent models will be developed and discussed here.

3.2 Estimating constituents properties from Eshelby-Kröner self-consistent or Mori-Tanaka inverse scale transition models

3.2.1 Application of Eshelby-Kröner self-consistent framework to the identification of the pseudo-macroscopic properties of one constituent embedded in a two-constituents composite material

The pseudomacroscopic stiffness tensor of the reinforcements can be deduced from the inversion of the Eshelby-Kröner main homogenization form over the constituents elastic properties (1) as follows :

$$\mathbf{L^r} = \frac{1}{v^r}\mathbf{L^I} : \left[\mathbf{E^I} : \left(\mathbf{L^r} - \mathbf{L^I}\right) + \mathbf{I}\right] - \frac{v^m}{v^r}\mathbf{L^m} : \left[\mathbf{E^I} : \left(\mathbf{L^m} - \mathbf{L^I}\right) + \mathbf{I}\right]^{-1} : \left[\mathbf{E^I} : \left(\mathbf{L^r} - \mathbf{L^I}\right) + \mathbf{I}\right] \qquad (18)$$

The application of this equation implies that both the macroscopic stiffness and the pseudomacroscopic mechanical behaviour of the matrix is perfectly determined. The elastic stiffness of the matrix constituting the composite ply will be assumed to be identical to the elastic stiffness of the pure single matrix, deduced in practice from measurements performed on bulk samples made up of pure matrix. It was demonstrated in (Fréour et al., 2002) that this assumption was not leading to significant errors in the case that polycrystalline multi-phase samples were considered. The similarities existing between multi-phase polycrystals and polymer based composites suggest that this assumption should be suitable in the present context, at least when scale factors do not occur. Nevertheless, in the case that significant edge effects, due for instance to a reduced thickness of the matrix layer constituting the composite ply, might be expected to occur, the identification of the ply embedded matrix elastic properties to those of the corresponding bulk material would not systematically be appropriate. Consequently, the application of inverse form (18) given above could lead to an erroneous estimation of the reinforcements elastic stiffness. Moreover, identification based on such inverse homogenization methods are sensitive to both the precise knowledge of the constituents volume fractions (i.e. v^m and v^r) and to the presence of porosities (which lowers the effective stiffness $\mathbf{L^I}$ of the composite ply).
An expression, analogous to above-relation (18) can be found for the elastic stiffness of the matrix, through the following replacement rules over the superscripts/subscripts: $\mathrm{m} \to \mathrm{r}, \mathrm{r} \to \mathrm{m}$. Nevertheless, the situation, where the properties of the reinforcements are known, when those of the matrix are unknown is highly improbable.

The pseudomacroscopic coefficients of moisture expansion of the matrix can be deduced from the inversion of the homogenization form (2) as follows :

$$\boldsymbol{\beta}^{\mathbf{m}} = \frac{1}{v^m \, \Delta C^m}\mathbf{L^m}^{-1} : \left(\mathbf{L^m} + \mathbf{L^I} : \mathbf{R^I}\right) : \mathbf{G^m} \qquad (19)$$

where $\mathbf{G^m}$ writes :

$$\mathbf{G^m} = \Delta C^I \left\langle \left(\mathbf{L^i} + \mathbf{L^I} : \mathbf{R^I} \right)^{-1} : \mathbf{L^I} \right\rangle_{i=r,m} : \boldsymbol{\beta}^{\mathbf{I}} - v^r \left(\mathbf{L^r} + \mathbf{L^I} : \mathbf{R^I} \right)^{-1} : \mathbf{L^r} : \boldsymbol{\beta}^{\mathbf{r}} \Delta C^r \quad (20)$$

An expression, analogous to above-relation (19) can also be found for the coefficients of moisture expansion of a permeable reinforcement type, through the following replacement rules over the superscripts/subscripts: $m \to r, r \to m$.

In the particular case, where impermeable reinforcements are present in the composite structure, the coefficients of moisture expansion of the matrix simplifies as follows (an extensive study of this very question was achieved in Jacquemin et al., 2005):

$$\boldsymbol{\beta}^{\mathbf{m}} = \frac{\Delta C^I}{v^m \, \Delta C^m} \mathbf{L^m}^{-1} : \left(\mathbf{L^m} + \mathbf{L^I} : \mathbf{R^I} \right) : \left\langle \left(\mathbf{L^i} + \mathbf{L^I} : \mathbf{R^I} \right)^{-1} : \mathbf{L^I} \right\rangle_{i=r,m} : \boldsymbol{\beta}^{\mathbf{I}} \quad (21)$$

The pseudomacroscopic coefficients of thermal expansion of the matrix can be deduced from the inversion of the homogenization form (3) as follows:

$$\mathbf{M^m} = \mathbf{L^m}^{-1} : \left(\mathbf{L^m} + \mathbf{L^I} : \mathbf{R^I} \right) : \left[\left\langle \left(\mathbf{L^i} + \mathbf{L^I} : \mathbf{R^I} \right)^{-1} : \mathbf{L^I} \right\rangle_{i=r,m} : \mathbf{M^I} - v^r \left(\mathbf{L^r} + \mathbf{L^I} : \mathbf{R^I} \right)^{-1} : \mathbf{L^r} : \mathbf{M^r} \right] \quad (22)$$

Form (22) can be easily rewritten for expressing the coefficients of thermal expansion of the reinforcements, using the same replacement rules over the superscripts/subscripts: $m \to r, r \to m$, than for the previous cases.

3.2.2 Application of Mori-Tanaka estimates to the identification of the pseudo-macroscopic properties of one constituent embedded in a two-constituents composite material

3.2.2.1 Inverse Mori-Tanaka elastic model

In the present work, it is be considered, that the reinforcements are surrounded by the matrix, thus, $\mathbf{T^m = I}$ and (11) develops as follows:

$$\mathbf{L^I} = \left(v^m \, \mathbf{L^m} + v^r \, \mathbf{L^r} : \mathbf{T^r} \right) : \left(v^m \, \mathbf{I} + v^r : \mathbf{T^r} \right)^{-1} \quad (23)$$

Thus, from (11) two alternate equations are obtained for identifying the pseudo-macroscopic stiffness of the composite ply constituents:

- On the first hand, the elastic properties of the matrix satisfies

$$\mathbf{L^m} = \mathbf{L^I} + \frac{1 - v^m}{v^m} \left(\mathbf{L^I} - \mathbf{L^r} \right) : \mathbf{T^r} \quad (25)$$

Equation (25) is an implicit equation since both its left and right hand sides involve the researched stiffness tensor $\mathbf{L^m}$.

- whereas, on the second hand, the elastic stiffness of the reinforcements respects

$$\mathbf{L^r} = \mathbf{L^I} + \frac{v^m}{1 - v^m}\left(\mathbf{L^I} - \mathbf{L^m}\right) : \mathbf{T^r}^{-1} \tag{26}$$

For the same reasons as above (i.e. comments about equation (25)), expression (26) is an implicit relation. As a consequence, the need of an inverse modelling for achieving the identification of the elastic properties exhibited by any one constituent of a composite ply through Mori-Tanaka scale-transition approximate yields the loss of the main advantage of this very model over the more rigorous Eshelby-Kröner self-consistent approach: the opportunity to express analytical explicit relations instead of having to perform successive numerical calculations for solving implicit equations. Moreover, the general remarks about the sensitivity of identification methods to certain factors, expressed in subsection 3.2.1 are valid in the present context also.

3.2.2.2 Inverse Mori-Tanaka model for identifying coefficients of moisture of thermal expansion

Following the same line of reasoning as above, in the purely elastic case, one can inverse relation (12) in order to express the coefficients of moisture expansion of a constituent embedded in a composite ply according to Mori-Tanaka estimates, or its coefficients of thermal expansion, from the homogenization relation (13). In the case of the pure matrix, one gets:

$$\mathbf{M^m} = \frac{1}{v^m}\mathbf{L^m}^{-1} : \left[\left\langle \mathbf{L^i} : \mathbf{T^i} \right\rangle_{i=r,m} : \mathbf{M^I} - v^r \mathbf{L^r} : \mathbf{T^r} : \mathbf{M^r}\right] \tag{27}$$

$$\boldsymbol{\beta^m} = \frac{1}{v^m \Delta C^m}\mathbf{L^m}^{-1} : \left[\left\langle \mathbf{L^i} : \mathbf{T^i} \right\rangle_{i=r,m} : \boldsymbol{\beta^I} \Delta C^I - v^r \mathbf{L^r} : \mathbf{T^r} : \boldsymbol{\beta^r} \Delta C^r\right] \tag{28}$$

This last relation (valid for the general case of a possibly permeable reinforcement type) yields to the following simplified form if impermeable reinforcements are considered:

$$\boldsymbol{\beta^m} = \frac{1}{v^m \Delta C^m}\mathbf{L^m}^{-1} : \left\langle \mathbf{L^i} : \mathbf{T^i} \right\rangle_{i=r,m} : \boldsymbol{\beta^I} \Delta C^I \tag{29}$$

Due to the localization procedure which does not treat in an equivalent way the embedding matrix and the embedded inclusions (reinforcements) in the point of view of Mori-Tanaka scale-transition approach, the inverse forms satisfied by the coefficients of thermal expansion and coefficients of moisture expansion of the reinforcements are not anymore deduced from the above-relations established for the matrix through simple replacement rules. Actually, unlike the inverse forms obtained according to Eshelby-Kröner self-consistent model, Mori-Tanaka model yields non-equivalent inverse forms for the matrix one the one hand and for the

reinforcements, on the second hand. The expressions, required for identifying the thermal or hygroscopic properties of reinforcements within Mori-Tanaka model are:

$$\mathbf{M^r} = \frac{1}{v^r}\mathbf{T^r}^{-1} : \mathbf{L^r}^{-1} : \left[\left\langle \mathbf{L^i} : \mathbf{T^i} \right\rangle_{i=r,m} : \mathbf{M^I} - v^m \mathbf{L^m} : \mathbf{M^m} \right] \tag{30}$$

$$\boldsymbol{\beta^r} = \frac{1}{v^r \Delta C^r}\mathbf{T^r}^{-1} : \mathbf{L^r}^{-1} : \left[\left\langle \mathbf{L^i} : \mathbf{T^i} \right\rangle_{i=r,m} : \boldsymbol{\beta^I} \Delta C^I - v^m \mathbf{L^m} : \boldsymbol{\beta^m} \Delta C^m \right] \tag{31}$$

3.3 Examples of properties identification in composite structures using inverse scale transition methods

3.3.1 Determination of reinforcing fibers elastic properties

The literature often provides elastic properties of carbon-fiber reinforced epoxies (see for instance Sai Ram and Sinha, 1991), that can be used in order to apply inverse scale transition model and thus identify the properties of the reinforcing fibers, as an example. Table 2 of the present work summarizes the previously published data for an unidirectional composite designed for aeronautic applications, containing a volume fraction v^r=0.60 of reinforcing fibers. In order to achieve the calculations, according to relations (18) or (26) depending on whether Eshelby-Kröner model or Mori-Tanaka approximation, input values are required for the pseudo-macroscopic properties of the epoxy matrix constituting the composite ply. The elastic constants considered for this purpose are listed in Table 3 (from Herakovich, 1998). Both the above-cited inverse scale transition methods have been applied. The obtained results are provided in Table 4, where they are compared to typical values, reported in the literature, for high-strength reinforcing fibers (Herakovich, 1998). It is shown that a very good agreement between the two inverse models is obtained. Moreover, the calculated values are similar to those expected for typical reinforcements according to the literature. Nevertheless, some discrepancies between the identified moduli do exist, especially for G_{12}^r (that corresponds to L_{55}^r stiffness component). Actually, the value deduced for this component through Mori-Tanaka inverse model deviates from both the expected properties and the estimations of Eshelby-Kröner model. This deviation, occurring for this very component, is obviously directly related to the discrepancies previously underlined in subsection 2.5 where the question of comparing the homogenization relations of the two scale transition methods presented in this paper, was investigated.

3.3.2 Determination of AS4/3501-6 matrix Coefficients of Moisture Expansion

Macroscopic values of the Coefficients of Moisture Expansion are sometimes available, contrary to the corresponding pure epoxy resin CME. Simulations were performed in the cas e of an AS4/3501-6 composite, with a reinforcing fiber volume fraction v^r=0.60. The calculations were achieved using the elastic properties given in Table 5, and the macroscopic coefficients of moisture expansion listed in Table 6. The same table summarizes the results obtained with both inverse Eshelby-Kröner self-consistent model (21) and Mori-Tanaka estimates (29) assuming a moisture content $\frac{\Delta C^m}{\Delta C^I} = 3.125$ (the ratio between composite and resin densities being 1.25 in this material, the moisture content ratio assumed in the present

study corresponds to the maximum expected value), in the case that impermeable reinforcements are considered. According to Table 6, a very good agreement is obtained between the two inverse models. This result is compatible with the homogenisation calculation previously achieved in subsection 2.5: for such a volume fraction of reinforcements, Eshelby-Kröner and Mori-Tanaka models provide identical macroscopic coefficients of moisture expansion from the pseudomacroscopic data. As a consequence, the corresponding inverse forms (21) and (29) yields the same estimation for the pseudomacroscopic CME of the matrix constituting the composite ply.

4- From the numerical model to analytical solutions for estimating the pseudo-macroscopic mechanical states

4.1 Introduction

It was extensively discussed in previously published works (the interested reader can, for instance refer to Benveniste, 1987 and Fréour et al., 2006a, where the question is addressed), that Mori and Tanaka constitutive assumptions were not suitable for a reliable estimation of the localization of the macroscopic mechanical states within the constituents of typical composites conceived for engineering applications, which often present a significant volume fraction of reinforcements. As a consequence, only Eshelby-Kröner approach will be considered in the present section.

4.2 Numerical SC model extended to a thermo-hygro-elastic load

Within Kröner and Eshelby self-consistent framework, the hygrothermal dilatation generated by a moisture content increment ΔC^i is treated as a transformation strain exactly like the thermal dilatation occurring after a temperature increment ΔT^i (that last case was extensively discussed in the literature, see for example Kocks et al., 1998). Thus, the pseudo-macroscopic stresses $\boldsymbol{\sigma}^{\mathbf{i}}$ in the considered constituent (i.e. i=r or i=m) are given by:

$$\boldsymbol{\sigma}^{\mathbf{i}} = \mathbf{L}^{\mathbf{i}} : \left(\boldsymbol{\varepsilon}^{\mathbf{i}} - \mathbf{M}^{\mathbf{i}} \Delta T^{i} - \boldsymbol{\beta}^{\mathbf{i}} \Delta C^{i} \right) \tag{32}$$

Where, $\boldsymbol{\varepsilon}$ stands for the strain tensor. In general case, the moisture content differs at macroscopic scale and pseudo-macroscopic scale, contrary to the temperature. Actually, the reinforcements generally do not absorb moisture. In consequence, the mass of water contained by the composite is: either found in the matrix, locally trapped in porosities (Mensitieri et al., 1995) or located where fiber debonding occurs.
Replacing the superscripts ^{i} by ^{I} in (32) leads to the stress-strain relation that holds at macroscopic scale.

$$\boldsymbol{\sigma}^{\mathbf{I}} = \mathbf{L}^{\mathbf{I}} : \left(\boldsymbol{\varepsilon}^{\mathbf{I}} - \mathbf{M}^{\mathbf{I}} \Delta T^{I} - \boldsymbol{\beta}^{\mathbf{I}} \Delta C^{I} \right) \tag{33}$$

The so-called “scale-transition relation” enabling to determine the local stresses and strains from the macroscopic mechanical states was demonstrated in a fundamental work, starting from the assumption that the elementary inclusions (here the matrix and the fiber) have ellipsoidal shapes (Eshelby, 1957):

$$\boldsymbol{\sigma}^{\mathbf{i}} - \boldsymbol{\sigma}^{\mathbf{I}} = -\mathbf{L}^{\mathbf{I}} : \mathbf{R}^{\mathbf{I}} : \left(\boldsymbol{\varepsilon}^{\mathbf{i}} - \boldsymbol{\varepsilon}^{\mathbf{I}} \right) \tag{34}$$

Actually, (34) is not very useful, because both the unknown pseudo-macroscopic stresses and strains appear. Nevertheless, combining (32-34) enables to find the following expression for the pseudo-macroscopic strain (the demonstration is available in Jacquemin et al., 2005 and Fréour et al., 2003b):

$$\boldsymbol{\varepsilon}^{\mathbf{i}} = \left(\mathbf{L}^{\mathbf{i}} + \mathbf{L}^{\mathbf{I}} : \mathbf{R}^{\mathbf{I}}\right)^{-1} : \left[\left(\mathbf{L}^{\mathbf{I}} + \mathbf{L}^{\mathbf{I}} : \mathbf{R}^{\mathbf{I}}\right).\boldsymbol{\varepsilon}^{\mathbf{I}} + \left(\mathbf{L}^{\mathbf{i}} : \mathbf{M}^{\mathbf{i}} - \mathbf{L}^{\mathbf{I}} : \mathbf{M}^{\mathbf{I}}\right)\Delta T + \mathbf{L}^{\mathbf{i}} : \boldsymbol{\beta}^{\mathbf{i}}\Delta C^{i} - \mathbf{L}^{\mathbf{I}} : \boldsymbol{\beta}^{\mathbf{I}}\Delta C^{I}\right] \quad (35)$$

In relation (35), the classical replacement rule $\Delta T^{i}=\Delta T^{I}=\Delta T$ was introduced (i.e. the temperature field is considered to be uniform within the considered ply).
Moreover, it was established in (Hill, 1967), that the self-consistent model was compatible with the following volume averages on both pseudo-macroscopic stresses and strains:

$$\left\langle \boldsymbol{\sigma}^{\mathbf{i}} \right\rangle_{i=r,m} = \boldsymbol{\sigma}^{\mathbf{I}} \qquad \left\langle \boldsymbol{\varepsilon}^{\mathbf{i}} \right\rangle_{i=r,m} = \boldsymbol{\varepsilon}^{\mathbf{I}} \quad (36)$$

For a given applied macroscopic thermo-hygro-elastic load $\{\boldsymbol{\sigma}^{\mathbf{I}}, \Delta C^{I,} \Delta T\}$ one can easily determine $\boldsymbol{\varepsilon}^{\mathbf{I}}$ through (33), provided that the effective elastic behaviour $\mathbf{L}^{\mathbf{I}}$ of the ply has been calculated using either the homogenization procedure corresponding to Eshelby-Kröner model or the corresponding Mori-Tanaka alternate solution (see previous developments provided in section 2 above). Then, the pseudo-macroscopic strains are determined through (35).

4.3 Analytical expression for calculating the mechanical states experienced by the constituents of fiber-reinforced composites according to Eshelby-Kröner model

The main impediment requiring to be overcome in order to achieve closed-forms from relation (35) is the determination of Morris' tensor $\mathbf{E}^{\mathbf{I}}$. Actually, according to the integrals appearing in relation (8), this tensor will admit only numerical solutions in most cases.

However, some analytical forms for Morris' tensor are actually available in the literature; the interested reader can for instance refer to (of Mura, 1982; Kocks et al., 1998; or Qiu and Weng 1991). Nevertheless, these forms were established considering either spherical, disc-shaped of fiber-shaped inclusions embedded in an ideally isotropic macroscopic medium, that is incompatible with the strong elastic anisotropy exhibited by fiber-reinforced composites at macroscopic scale (Tsai and Hahn, 1987).
In the case of carbon-epoxy composites, a transversely isotropic macroscopic behaviour being coherent with fiber shape is actually expected (and predicted by the numerical computations). Assuming that the longitudinal (subscripted $_1$) axis is parallel to fiber axis, one obtains the following conditions for the semi-lengths of the microstructure representative ellipsoid: $a_1 \to \infty$, $a_2=a_3$. Moreover, the macroscopic elastic stiffness should satisfy : $L^{I}_{11} \neq L^{I}_{12} \neq L^{I}_{22} \neq L^{I}_{23} \neq L^{I}_{44} \neq L^{I}_{55}$. Now, it is obvious, that these additional hypotheses lead to drastic simplifications of Morris' tensor (8), in the case that fiber morphology is considered for the reinforcements. The line of reasoning required to achieve the writing of analytical expressions for Morris' tensor is extensively presented in (Welzel et al., 2005;

Fréour et al., 2005). Actually, one obtains (in contracted notation i.e, E_{ij}^{I} components are given here):

$$\mathbf{E^I} = \begin{bmatrix} 0 & 0 & 0 & 0 & 0 & 0 \\ 0 & \dfrac{3}{8L_{22}^{I}} + \dfrac{1}{4L_{22}^{I} - 4L_{23}^{I}} & \dfrac{L_{22}^{I} + L_{23}^{I}}{8L_{22}^{I}L_{23}^{I} - 8L_{22}^{I^2}} & 0 & 0 & 0 \\ 0 & \dfrac{L_{22}^{I} + L_{23}^{I}}{8L_{22}^{I}L_{23}^{I} - 8L_{22}^{I^2}} & \dfrac{3}{8L_{22}^{I}} + \dfrac{1}{4L_{22}^{I} - 4L_{23}^{I}} & 0 & 0 & 0 \\ 0 & 0 & 0 & \dfrac{1}{8L_{22}^{I}} + \dfrac{1}{4L_{22}^{I} - 4L_{23}^{I}} & 0 & 0 \\ 0 & 0 & 0 & 0 & \dfrac{1}{8L_{55}^{I}} & 0 \\ 0 & 0 & 0 & 0 & 0 & \dfrac{1}{8L_{55}^{I}} \end{bmatrix} \tag{37}$$

In fact, the epoxy matrix is usually isotropic, so that three components only have to be considered for its elastic constants: L_{11}^{m}, L_{12}^{m} and L_{44}^{m}. One moisture expansion coefficient is sufficient to describe the hygroscopic behaviour of the matrix: β_{11}^{m}.
In the case of the carbon fibers, a transverse isotropy is generally observed. Thus, the corresponding elasticity constants depend on the following components: $L_{11}^{r}, L_{12}^{r}, L_{22}^{r}, L_{23}^{r}, L_{44}^{r}$, and L_{55}^{r}. Moreover, since the carbon fiber does not absorb water, its CME β_{11}^{r} and β_{22}^{r} will not be involved in the mechanical states determination. Introducing these additional assumptions in (35), and taking into account the form (37) obtained for Morris' tensor, one can deduce the following strain tensors for both the matrix and the fibers:

$$\varepsilon^{i} = \begin{bmatrix} \varepsilon_{11}^{i} & \varepsilon_{12}^{i} & \varepsilon_{13}^{i} \\ \varepsilon_{12}^{i} & \varepsilon_{22}^{i} & \varepsilon_{23}^{i} \\ \varepsilon_{13}^{i} & \varepsilon_{23}^{i} & \varepsilon_{33}^{i} \end{bmatrix} \tag{38}$$

where, in the case of the matrix,

$$
\begin{cases}
\varepsilon_{11}^{m} = \varepsilon_{11}^{I} \\
\varepsilon_{12}^{m} = \dfrac{2\,L_{55}^{I}\,\varepsilon_{12}^{I}}{L_{55}^{I}+L_{44}^{m}} \\
\varepsilon_{13}^{m} = \dfrac{2\,L_{55}^{I}\,\varepsilon_{13}^{I}}{L_{55}^{I}+L_{44}^{m}} \\
\varepsilon_{22}^{m} = \dfrac{N_1^{m}+N_2^{m}+N_3^{m}+N_4^{m}+N_5^{m}}{D_1^{m}} \\
\varepsilon_{23}^{m} = \dfrac{2\,L_{22}^{I}\left(L_{22}^{I}-L_{23}^{I}\right)\varepsilon_{23}^{I}}{2\,L_{22}^{I^2}+L_{23}^{I}\left(L_{44}^{I}-L_{44}^{m}\right)+L_{22}^{I}\left(3\,L_{44}^{m}-2\,L_{23}^{I}-3\,L_{44}^{m}\right)} \\
\varepsilon_{33}^{m} = \varepsilon_{22}^{m} - 4\,L_{22}^{I}\,\dfrac{\left(L_{22}^{I}-L_{23}^{I}\right)\left(\varepsilon_{22}^{I}-\varepsilon_{33}^{I}\right)}{L_{22}^{I^2}+3\,L_{22}^{I}\left(L_{11}^{m}-L_{12}^{m}\right)-L_{23}^{I}\left(L_{11}^{m}+L_{23}^{I}-L_{12}^{m}\right)}
\end{cases}
\tag{39}
$$

$$
\begin{cases}
N_1^{m} = \left(L_{11}^{m}+2L_{12}^{m}\right)\left(\beta_{11}^{m}\,\Delta C^{m}+M_{11}^{m}\,\Delta T\right) \\
N_2^{m} = -L_{12}^{I}\left(\beta_{11}^{I}\Delta C^{I}+M_{11}^{I}\Delta T\right)-\left(L_{22}^{I}+L_{23}^{I}\right)\left(\beta_{22}^{I}\Delta C^{I}+M_{33}^{I}\Delta T\right) \\
N_3^{m} = \left(L_{12}^{I}-L_{12}^{m}\right)\varepsilon_{11}^{I} \\
N_4^{m} = L_{22}^{I}\,\dfrac{L_{22}^{I}\left(5\,L_{11}^{m}-L_{12}^{m}+3\,L_{22}^{I}\right)-L_{23}^{I}\left(3\,L_{11}^{m}+L_{12}^{m}+4\,L_{22}^{I}\right)+L_{23}^{I^2}}{\left(3\,L_{22}^{I}-L_{23}^{I}\right)\left(L_{11}^{m}-L_{12}^{m}\right)+L_{22}^{I^2}-L_{23}^{I^2}}\,\varepsilon_{22}^{I} \\
N_5^{m} = L_{22}^{I}\,\dfrac{L_{22}^{I}\left(L_{11}^{m}-5\,L_{12}^{m}-L_{22}^{I}\right)+L_{23}^{I}\left(L_{11}^{m}+3\,L_{12}^{m}+4\,L_{22}^{I}\right)-3\,L_{23}^{I^2}}{\left(3\,L_{22}^{I}-L_{23}^{I}\right)\left(L_{11}^{m}-L_{12}^{m}\right)+L_{22}^{I^2}-L_{23}^{I^2}}\,\varepsilon_{33}^{I} \\
D_1^{m} = L_{11}^{m}+L_{12}^{m}+L_{22}^{I}-L_{23}^{I}
\end{cases}
\tag{40}
$$

The pseudo-macroscopic stress tensors are deduced from the strains using (32). Thus, in the matrix, one will have:

$$
\sigma^{m} = \begin{bmatrix}
\sigma_{11}^{m} & 2\,L_{44}^{m}\varepsilon_{12}^{m} & 2\,L_{44}^{m}\varepsilon_{13}^{m} \\
2\,L_{44}^{m}\varepsilon_{12}^{m} & \sigma_{22}^{m} & 2\,L_{44}^{m}\varepsilon_{23}^{m} \\
2\,L_{44}^{m}\varepsilon_{13}^{m} & 2\,L_{44}^{m}\varepsilon_{23}^{m} & \sigma_{33}^{m}
\end{bmatrix}
\tag{41}
$$

$$\text{with } \begin{cases} \sigma_{11}^{m} = L_{11}^{m}\left(\varepsilon_{11}^{m} - M_{11}^{m}\,\Delta T\right) + L_{12}^{m}\left(\varepsilon_{22}^{m} + \varepsilon_{33}^{m} - 2\,M_{11}^{m}\,\Delta T\right) - \beta_{11}^{m}\left(L_{11}^{m} + 2\,L_{12}^{m}\right)\Delta C^{m} \\ \sigma_{22}^{m} = L_{11}^{m}\left(\varepsilon_{22}^{m} - M_{11}^{m}\,\Delta T\right) + L_{12}^{m}\left(\varepsilon_{11}^{m} + \varepsilon_{33}^{m} - 2\,M_{11}^{m}\,\Delta T\right) - \beta_{11}^{m}\left(L_{11}^{m} + 2\,L_{12}^{m}\right)\Delta C^{m} \\ \sigma_{33}^{m} = L_{11}^{m}\left(\varepsilon_{33}^{m} - M_{11}^{m}\,\Delta T\right) + L_{12}^{m}\left(\varepsilon_{11}^{m} + \varepsilon_{22}^{m} - 2\,M_{11}^{m}\,\Delta T\right) - \beta_{11}^{m}\left(L_{11}^{m} + 2\,L_{12}^{m}\right)\Delta C^{m} \end{cases} \quad (42)$$

The local mechanical states in the fiber are provided by Hill's strains and stresses average laws (36):

$$\boldsymbol{\varepsilon}^{\mathbf{r}} = \frac{1}{v^{r}}\boldsymbol{\varepsilon}^{\mathbf{I}} - \frac{v^{m}}{v^{r}}\boldsymbol{\varepsilon}^{\mathbf{m}} \quad (43)$$

$$\boldsymbol{\sigma}^{\mathbf{r}} = \frac{1}{v^{r}}\boldsymbol{\sigma}^{\mathbf{I}} - \frac{v^{m}}{v^{r}}\boldsymbol{\sigma}^{\mathbf{m}} \quad (44)$$

4.4 Examples of multi-scale stresses estimations in composite structures : T300-N5208 composite pipe submitted to environmental conditions

4.4.1 Macroscopic analysis

4.4.1.1 Moisture concentration

Consider an initially dry, thin uni-directionally reinforced composite pipe, whose inner and outer radii are *a* and *b* respectively, and let the laminate be exposed to an ambient fluid with boundary concentration c_0. The macroscopic moisture concentration, $c^I(r,t)$, is solution of the following system with Fick's equation (45), where D^I is the transverse diffusion coefficient of the composite. Boundary and initial conditions are described in (46):

$$\frac{\partial c^{I}}{\partial t} = D^{I}\left[\frac{\partial^{2} c^{I}}{\partial r^{2}} + \frac{1}{r}\frac{\partial c^{I}}{\partial r}\right],\ a<r<b \quad (45)$$

$$\begin{cases} c^{I}(a,t) = c_0 \text{ and } c^{I}(b,t) = c_0 \\ c^{I}(r,0) = 0 \end{cases} \quad (46)$$

Applying the Laplace transform to the latter system and using the residue theory to express the solution in time space (Crank, 1975), we finally obtain the macroscopic moisture concentration:

$$c^{I}(\bar{r},\tau) = c_0 + \sum_{m=1}^{\infty} \frac{2\exp(-\omega^{2}{}_{m}\tau)}{\omega_m \Delta'_u(\omega_m)}\left\{ A_m J_0(\omega_m \bar{r}) + B_m Y_0(\omega_m \bar{r}) \right\} \quad (47)$$

where J_0 and Y_0 are Bessel's functions of order zero, Δ_u is the determinant of 2*2 matrix $[a]$. A_m and B_m are determinants of matrices deduced from $[a]$ by substituting respectively column 1 and 2 by the constant vector $\{g\}$. $\Delta'_u(\omega_m)$ is the derivative of Δ_u with respect to

ω calculated for ω_m the mth positive root of Δ_u. $\bar{r}$ and τ are defined by the relations $\bar{r} = r/b$ and $\tau = (D^I t)/b^2$.

Furthermore, the elements of $[a]$ and $\{g\}$ are: $a_{11} = J_0(\omega\bar{a})$, $a_{12} = Y_0(\omega\bar{a})$, $a_{21} = J_0(\omega)$, $a_{22} = Y_0(\omega)$, $g_1 = c_0$, $g_2 = c_0$.

4.4.1.2 Macroscopic stresses

At the initial time, let us assume that the pipe is stress free. Therefore, the hygro-elastic orthotropic behaviour writes as follows in (48-49), where $\boldsymbol{\beta}^{\mathbf{I}}$ and $\mathbf{L}^{\mathbf{I}}$ are respectively the in-plane tensors of hygroscopic expansion coefficients and moduli. Those tensors are assumed to be material constants.

$$\begin{Bmatrix} \sigma_{11}^I \\ \sigma_{22}^I \\ \sigma_{33}^I \\ \tau_{12}^I \end{Bmatrix} = \begin{bmatrix} L_{11}^I & L_{12}^I & L_{12}^I & 0 \\ L_{12}^I & L_{22}^I & L_{23}^I & 0 \\ L_{12}^I & L_{23}^I & L_{22}^I & 0 \\ 0 & 0 & 0 & L_{55}^I \end{bmatrix} \begin{Bmatrix} \varepsilon_{11}^I - \beta_{11}^I \Delta C^I \\ \varepsilon_{22}^I - \beta_{22}^I \Delta C^I \\ \varepsilon_{33}^I - \beta_{22}^I \Delta C^I \\ \gamma_{12}^I - \beta_{12}^I \Delta C^I \end{Bmatrix} \tag{48}$$

$$\begin{Bmatrix} \tau_{32}^I \\ \tau_{13}^I \end{Bmatrix} = \begin{bmatrix} L_{44}^I & 0 \\ 0 & L_{55}^I \end{bmatrix} \begin{Bmatrix} \gamma_{32}^I \\ \gamma_{13}^I \end{Bmatrix} \tag{49}$$

with, $\Delta C^I = \dfrac{c^I}{\rho^I}$. c^I and ρ^I are respectively the macroscopic moisture concentration and the mass density of the dry material.
To solve the hygromechanical problem, it is necessary to express the strains versus the displacements along with the compatibility and equilibrium equations.

Introducing a characteristic modulus L_0, we introduce the following dimensionless variables:

$$\bar{\boldsymbol{\sigma}}^{\mathbf{I}} = \boldsymbol{\sigma}^{\mathbf{I}} / L_0, \bar{\mathbf{L}}^{\mathbf{I}} = \mathbf{L}^{\mathbf{I}} / L_0, (\bar{w}^I, \bar{u}^I, \bar{v}^I) = (w^I, u^I, v^I) / b.$$

Displacements with respect to longitudinal and circumferencial directions, respectively $\bar{u}^I(\bar{x},\bar{r})$ and $\bar{v}^I(\bar{x},\bar{r})$ are then deduced:

$$\begin{cases} \bar{u}^I(\bar{x},\bar{r}) = R_1 \bar{x} \\ \bar{v}^I(\bar{x},\bar{r}) = R_2 \bar{x}\bar{r} \\ R_1, R_2 \text{ are constants}. \end{cases} \tag{50}$$

It is worth noticing that the displacements $\bar{u}^I(\bar{x},\bar{r})$ and $\bar{v}^I(\bar{x},\bar{r})$ do not depend on the moisture concentration field. Finally, to obtain the through-thickness or radial component of the displacement $\bar{w}^I$, we shall consider in the following the analytical transient concentration (47).

The radial component of the displacement field $\overline{w}^I$ satisfies the following equation:

$$\bar{r}^2 \frac{\partial^2 \overline{w}^I}{\partial \bar{r}^2} + \bar{r} \frac{\partial \overline{w}^I}{\partial \bar{r}} - \overline{w}^I = \frac{K_1 \bar{r}^2 \frac{\partial \Delta C^I}{\partial \bar{r}}}{\overline{L}^I_{22}} \tag{51}$$

with, $K_1 = \overline{L}^I_{12} \beta^I_{11} + \overline{L}^I_{23} \beta^I_{22} + \overline{L}^I_{22} \beta^I_{22}$

It is shown that the general solution of equation (51) writes as the sum of a solution of the homogeneous equation and of a particular solution (Jacquemin et Vautrin, 2002).

$$\overline{w}^I(\bar{r}) = R_3 \bar{r} + \frac{R_4}{\bar{r}} -$$

$$\sum_{m=1}^{\infty} \frac{2\exp(-\omega_m^2 \tau)}{\omega_m \Delta'_u(\omega_m)} \frac{K_1}{\overline{L}^I_{22}} \left[A_i \sum_{k=0}^{\infty} \frac{(-1)^k (\frac{1}{2})^{2k+1} (\omega_m)^{2k+2}}{k!(k+1)!} \frac{\bar{r}^{2k+3}}{((2k+3)^2 - 1)} + \frac{B_i}{\pi} \right\{$$

$$\sum_{k=0}^{\infty} \frac{(-1)^k (\frac{1}{2})^{2k+1} (\omega_m)^{2k+2}}{k!(k+1)!} [2\ln(\frac{1}{2}\omega_m) - \psi(k+1) - \psi(k+2)] \frac{\bar{r}^{(2k+3)}}{((2k+3)^2 - 1)} +$$

$$2 \sum_{k=0}^{\infty} \frac{(-1)^k (\frac{1}{2})^{2k+1} (\omega_m)^{2k+2}}{k!(k+1)!} [\frac{\ln(\bar{r}) \bar{r}^{2k+3}}{((2k+3)^2 - 1)} - \frac{2(2k+3)\bar{r}^{2k+3}}{((2k+3)^2 - 1)^2}] - \bar{r}\ln(\bar{r}) \left. \right\} \left. \right]$$

Finally, the displacement field depends on four constants to be determined : R_i for i=1..4. These four constants result from the following conditions :

- global force balance of the cylinder;
- nullity of the normal stress on the two lateral surfaces.

4.4.2 Numerical simulations of internal stresses in T300/5208 composite laminated pipes

4.4.2.1 Introduction

Thin laminated composite pipes, with thickness 4 mm, initially dry then exposed to an ambient fluid, made up of T300/5208 carbon-epoxy plies, with a fiber volume fraction v^r=0.6, were considered for the determination of both macroscopic stresses and moisture content as a function of time and space. The closed-form formalism used in order to determine the mechanical stresses and strains in each ply of the structure is described in subsection 4.4.1. This model ensures the calculation of the macroscopic moisture content, too.
When the equilibrium state is reached, the maximum moisture content of the neat resin may be estimated from the maximum moisture content of the composite. By assuming that the fibers do not absorb any moisture, ΔC^I and ΔC^m are related by expression (16) given by (Loos and Springer, 1981). In the case of T300/5208, since the ratio between composite and resin densities is 1.33 (due to the constituents properties listed in table 1), the maximum moisture content ratio given by (16) is about 3.33.

Figure 2 shows the time-dependent concentration profiles, resulting from the application of a boundary concentration c_0, as a function of the normalized radial distance from the inner radius r_{dim}. At the beginning of the diffusion process important concentration gradients occur near the external surfaces. The permanent concentration (noticed *perm* in the caption) holds with a constant value because of the symmetrical hygroscopic loading. The macroscopic mechanical states were calculated for two types of composites structures: a) a uni-directionnaly reinforced cylinder, and b) a [55°/-55°]$_S$ laminated cylinder.
Starting with the macroscopic stresses deduced from continuum mechanics, the local stresses in both the fiber and matrix were calculated either with the new analytical forms or the fully numerical model. The comparison between the two approaches is plotted on figures 3 and 4. These figures show the very good agreement between the numerical approach and the corresponding closed-forms solutions. The slight differences appearing are due to the small deviations on the components of Morris' tensor calculated using the two approaches. Actually, it is not possible to assume the quasi-infinite length of the fiber along the longitudinal axis in the case of the numerical approach, because the numerical computation of Morris' tensor is highly time-consuming. Thus, the numerical version of Eshelby-Kröner self-consistent model constitutes only an approximation of the real microstructure of the composite. In consequence, it seems that the new analytical forms, that are able to take into account the proper microstructure for the fibers, are not only more convenient, but also more reliable than the initially proposed numerical approach.

4.4.2.2 Interpretation of the simulations

The highest level of macroscopic tensile stress is reached for the uni-directional composite, in the transverse direction and in the central ply of the structure (figure 3). The transverse stresses exceed probably the macroscopic tensile strength in this direction. The choice of a [+55°/-55°]$_S$ laminated allows to reduce the macroscopic stress in the transverse direction. Nevertheless, a high shear stress rises along the time in the fibers of the central ply of such a structure (figure 3).
Moreover, the figure 4 shows that the micro-mechanical model always predict a very high compressive stress in the matrix of the inner ply whatever the laminate studied (the macroscopic stress is negligible in the radial direction because thin structures are considered). These local stresses could help to explain damage occurrence in the surface of composite structures in fatigue.
This work demonstrates the complementarities of continuum mechanics and micro-mechanical models for the prediction of a possible damage in composite structures submitted to hygro-elastic loads.
In the following section, the analytical expressions presented here for the localization of the macroscopic mechanical states within the plies constituents, will be inversed in order to achieve the identification of the strength of the constitutive matrix of a composite ply.

5- Identification of the local strength of the constitutive matrix of a composite ply

5.1 Introduction

Damage predictions are important for design and for guiding materials improvement for engineering applications. Composite structures encountered in engineering applications are designed to endure combined mechanical, thermal and hygroscopic loads during their service life. Besides, composite structures usually benefit from improved properties granted by a

multidirectional arrangement of their plies. The multiplicity of both possible loads and ply arrangements is not compatible with an extensive experimental investigation of composite structures damage. As a result, only uniaxial and pure shear test data of unidirectional composites are usually available in the literature. By consequence, the estimation of damage occurrence in composite structures requires introducing adapted failure criteria extending the available data to the combined loads and composite laminates considered for one particular application. Many published papers have dealt with this problem: see for instance (Tsai, 1987; Cuntze, 2003). Nevertheless, it is established for a long time, that in composite structures the damage initiates at microscopic scale, either (and most of time) in the matrix or (sometimes) in the fibers. The failure of a ply is thus closely related and explained by the failure of its microscopic constituents (Tsai, 1987; Cuntze, 2003; Fleck and Jelf, 1995; Kaddour et al., 2003; Khashaba, 2004). As a consequence, the reliable prediction of a possible damage occurrence of multi-directionnal laminates submitted to complex loading requires the knowledge of the microscopic failure criteria of the epoxy matrix and carbon fibers constituting the plies. Nevertheless, previous published works have emphasised the following remarkable result: the strength of the pure constituents (i.e. pure epoxy resin) strongly depends on the size of the sample, and especially on its thickness (Fiedler et al., 2001). Besides, the thickness of a ply in thin laminates has the magnitude of 150 microns, that is generally strongly weaker than the thickness of the samples tested for the experimental determination of the strength of the pure constituents. As a consequence, the experimental strengths of pure carbon fibers and epoxy matrices, determined on bulk specimen can hardly be directly used to properly estimate microscopic failure criteria in real structures. In particular, as shown for instance in (Garett and Bailey, 1977; Christensen and Rinde, 1979), the effect of the matrix on transverse failure of composite structures is of interest. The strain to failure of the pure matrix in uniaxial tension varied from 1.5 to 70 % whereas transverse strains to failure of corresponding fiber reinforced composites were dramatically smaller and varied only in the range 0.2 to 0.9%.
In the present study, an innovative method, dedicated to the determination of the microscopic stress/strain failure criteria of the epoxy matrix embedded in a composite structure is described. This method is based on the inversion of the analytical expressions presented in section 4.3. The present work describes developments relating the macroscopic failure envelopes to the microscopic ones. The conditions, indicated in already published literature, when the macroscopic failure can exclusively be attributed to matrix failure modes are taken into account as fundamental hypotheses of the present approach. The model enables the identification of both the strength coefficients and ultimate strength, so that the microscopic stress/strain failure envelopes can also be drawn. Applications to the case of two typical carbon/epoxy composites (T300/5208 and AS4/3501) are achieved: the failure conditions of the N5208 and 3501-6 epoxy resins will be determined and compared.

5.2 Determination of the local failure criterion of the matrix from the macroscopic strength data of the composite ply

5.2.1 Introduction – choice of a failure criterion

In this paper, failure is taken in the general sense previously defined in the literature, including fracture, but also yield, etc. Since this works aims applications to multidirectional structures submitted to triaxial stresses, general failure criteria are necessary to the description of the strength in both stress and strain spaces. Failure criteria serve important functions in the design and sizing of composite laminates. They should provide a convenient framework or model for mathematical operations. The framework should be the same for different

definitions of failures, such as the ultimate strength, endurance limit, or a working stress based on design or reliability considerations. However, the criteria are not intended to explain the mechanisms of failure, that can occur concurrently or sequentially. The quadratic criterion will be used in the present study: it includes interactions among the stress or strain components analogous to the Von Mises criterion for isotropic materials, and is compatible with the existence of strength having the properties, often met in the case that composite structures are considered, to be anisotropic and also possibly different in tension or compression. The criterion, expressed in stress space writes as follows :

$$F^i_{mnop}\sigma^i_{mn}\sigma^i_{op} + F^i_{mn}\sigma^i_{mn} = 1 \qquad (52)$$

where F stands for the strength parameters respectively expressed in stress space. The superscript ^{i} represents the scale considered for failure prediction (macroscopic: i=I or pseudomacroscopic: i=m or i=r).

In order to use the failure criteria (52) presented above, it is necessary to identify the quadratic (F^i_{mnop}) and linear (F^i_{mn}) strength parameters involved in the equation.

In the present work, for helping fixing the ideas, the simplified case of three-dimensional stresses and strains (for both macroscopic and microscopic scales), with a single shear component, usually met in multi-directional composite laminates submitted to mechanical loads (see examples given in Tsai, 1987) will be assumed to hold (i.e. $\sigma^i_{13} = \sigma^i_{23} = 0\,\text{MPa}$, $\varepsilon^i_{13} = \varepsilon^i_{23} = 0$, where the subscripts 1, 2 and 3 respectively denotes the directions parallel to the fiber axis, the transverse direction and the normal direction, in the orthogonal frame of reference of the considered ply). Besides, the strength should be unaffected by the direction or sign of the shear stress component σ^i_{12}: if shear stress is reversed, the strength should be kept constant. However, sign reversal for the longitudinal (σ^i_{11}) and transverse (σ^i_{22}) stresses components from tension to compression is expected to have a significant effect on both the macroscopic and microscopic strength of the composite. As a consequence, terms of equation (52) containing first-degree shear stress should be null. Finally, taking into account the definition chosen for the reference frame, and the properties of (at least) transverse isotropy exhibited at any (i.e. macroscopic or microscopic) scale in one ply, the strength parameters have to satisfy the following relations:

$$\begin{cases} F^i_{2222} = F^i_{3333}, \\ F^i_{1122} = F^i_{1133}, \\ F^i_{22} = F^i_{33}. \end{cases} \qquad (53)$$

Taking into account the above listed simplifications, equation (52) can be rewritten:

$$\begin{cases} 1 = F^i_{1111}\sigma^{i\,2}_{11} + 2F^i_{1212}\sigma^{i\,2}_{12} + F^i_{2222}\left(\sigma^{i\,2}_{22} + \sigma^{i\,2}_{33}\right) + 2F^i_{1122}\sigma^i_{11}\left(\sigma^i_{22} + \sigma^i_{33}\right) + 2F^i_{2233}\sigma^i_{22}\sigma^i_{33} + \\ \quad F^i_{11}\sigma^i_{11} + F^i_{22}\left(\sigma^i_{22} + \sigma^i_{33}\right) \end{cases} \tag{54}$$

5.2.2 Direct identification of the macroscopic strength parameters

Most of the unknown macroscopic strength parameters in stress space, appearing in equation (54) can be identified using information deduced from simple mechanical tests (uniaxial tension, compression or longitudinal shear tests Tsai, 1987):

$$F^I_{1111} = \frac{1}{X^I X^{I/}}, F^I_{2222} = \frac{1}{Y^I Y^{I/}}, F^I_{11} = \frac{1}{X^I} - \frac{1}{X^{I/}}, F^I_{22} = \frac{1}{Y^I} - \frac{1}{Y^{I/}}, F^I_{1212} = \frac{1}{2S^{I\,2}} \tag{55}$$

Where X^I and Y^I are respectively the longitudinal and transverse tensile stress strength, $X^{I/}$ and $Y^{I/}$ the longitudinal and transverse compressive stress strength, whereas S^I is the longitudinal shear stress.

The two unknown remaining terms, F^I_{1122} and F^I_{2233} are related to the interaction between two orthogonal stress components. The practical determination of these interaction terms requires performing biaxial tests, which are not as easy to achieve than uniaxial tests. As a consequence, the required data are often not available in the literature. There are, however, geometric and physical conditions fixing the mathematical form of the failure criterion (54): for instance, the failure envelope has to be closed so that the material cannot present infinite strength when submitted to any load. Let us introduce a dimensionless interaction term:

$$F^{i*}_{mmnn} = \frac{F^i_{mmnn}}{\sqrt{F^i_{mmmm}\,F^i_{nnnn}}} \tag{56}$$

For closed envelopes, the condition $-1 \le F^{i*}_{mmnn} \le 1$ has to be satisfied. But a more detailed theoretical study (see Liu and Tsai, 1998) reduces the admissible range to the domain [-1,0]. The same reference (Liu and Tsai, 1998) advises the choice of $F^{I*}_{mmnn} = -\frac{1}{2}$ for the macroscopic interaction term (which corresponds to the generalised Von Mises model), since this value is reasonable for a wide range of laminates. Taking into account this additional assumption in equation (56), the knowledge of F^I_{1111} and $F^I_{2222} = F^I_{3333}$ ensures the determination of the last two missing interaction terms F^I_{1122} and F^I_{2233}, in stress space.

One similar method could be applied in order to determine the macroscopic strength parameters expressed in strain space from the ultimate strains. Nevertheless, this method is not useful in practice since uniaxial strains are difficult to apply to a sample. Thus, the ultimate strains are generally deduced from the ultimate stresses: to reach this goal, one has to introduce the macroscopic properties, i.e. the stiffness tensor $\mathbf{L^I}$, in order to relate both failure

criteria through Hooke's law (33) expressed at macroscopic scale assuming a purely elastic load.

5.2.3 Identification of the microscopic strength parameter (of the matrix only) using an inverse method

From the standpoint of the structural designer, it is desirable to have failure criteria which are applicable at the level of the lamina, the laminate, and the structural component. Nevertheless, failure at macroscopic scale is often the consequence of an accumulation of micro-level failure events (Tsai, 1987; Liu and Tsai, 1998). Laminated materials typically exhibit many local failures prior to rupture. Thus, it is important to build up tools enabling to enhance the understanding of micro-level failure mechanisms in order to develop higher-strength materials. The ultimate goal is to have a failure theory that the designer can use with confidence under the most general structural configuration and loading conditions and that the developer of materials can use to design and fabricate new products to meet specific needs. In order to reach this goal, the estimation of microscopic strength criteria would be of a valuable help.
Since the epoxy resins involved in composite structures generally exhibit an isotropic hygro-mechanical behaviour, the microscopic strength criterion expressed in terms of stresses (54) simplifies as follows:

$$\begin{cases} 1 = F^{m}_{1111}\left(\sigma^{m2}_{11} + \sigma^{m2}_{22} + \sigma^{m2}_{33}\right) + 2F^{m}_{1212}\sigma^{m2}_{12} + 2F^{m}_{1122}\left[\sigma^{m}_{11}\left(\sigma^{m}_{22} + \sigma^{m}_{33}\right) + \sigma^{m}_{22}\sigma^{m}_{33}\right] \\ \quad + F^{m}_{11}\left(\sigma^{m}_{11} + \sigma^{m}_{22} + \sigma^{m}_{33}\right) \end{cases} \tag{57}$$

Thus, only four strength parameters have to be determined in order to enable failure predictions at microscopic scale: $F^{m}_{1111}, F^{m}_{1212}, F^{m}_{1122}, F^{m}_{11}$. Hypotheses being compatible with the experimental observations are necessary to build an inverse model enabling the determination of these four parameters from the corresponding, available from practical mechanical tests, macroscopic strength stress failure criterion.

The present work is focused on the development of modelling tools for the prediction of a possible damage occurrence in fiber-reinforced epoxy laminates submitted to mechanical loads. Actually, fibrous composite materials fail in a variety of mechanisms at the fiber/matrix microscopic scale. Besides, according to the literature, i) fiber-dominated failures usually occur when the plies are loaded in planes perpendicular to the fibers axis (longitudinal tension and compression), whereas ii) matrix-dominated failures often occur in the cases that the plies are loaded along the transverse and normal directions in tension and compression or when shear stresses are applied to the considered ply (Tsai, 1987; Liu and Tsai, 1998). Thus, matrix-dominated failure modes often occur in practice. As a consequence, the above listed i) and ii) statements will be used in order to identify microscopic strength parameters in stress and strain spaces for the matrix.
According to the developments of section 4, it is possible to derive the pioneering numerical self-consistent model of Kröner and Eshelby in order to find the relation between the macroscopic mechanical states and the researched corresponding microscopic stresses and strains existing in the matrix of a composite material.

In the present work, the strength parameters in either the matrix or the ply will be considered to remain independent from the magnitude of the applied mechanical load. Since the damage

envelope has been defined as the strain or stress threshold beyond which non-linearity occurs in the behaviour of the material at the scale concerned by damage, and in the case that a purely mechanical load is taken into account, the material is assumed to behave elastically until failure occurs. Now, in these conditions, both stress and strain ultimate strength are simultaneously reached, and satisfy either macroscopic elastic Hooke's law (33) or the corresponding microscopic relations that are deduced from (38-42), assuming $\Delta C^I = \Delta C^m = 0$ and $\Delta T^I = \Delta T^m = 0\,K$.

It will be assumed that macroscopic failure occurring in the transverse and normal directions, for a longitudinal stress $\sigma_{11}^I = 0\,MPa$, is governed by local failure of the matrix. Various macroscopic stress states, compatible with that last hypothesis, are taken on the macroscopic strength envelope (54), expressed in stress space and, finally implemented in the scale transition relations (38-42). This leads to the determination of microscopic mechanical stresses and strains states in the matrix, that are, according to our hypotheses, responsible for macroscopic damage governed by matrix failure. As a consequence, these local mechanical states should be compatible with the microscopic failure envelopes of the matrix as written in equations (57).
According to this relation, four, non equivalent, macroscopic stress states suffice to find the eight researched coefficients involved in (57): $F_{1111}^m, F_{1212}^m, F_{1122}^m, F_{11}^m$. The whole method required to perform such estimation is described on table 7. Actually, four macroscopic loading states taken on the stress failure envelope (defined on table 7) $\boldsymbol{\sigma}_{\mathbf{a}}^{\mathbf{I}}$, $\boldsymbol{\sigma}_{\mathbf{b}}^{\mathbf{I}}$, $\boldsymbol{\sigma}_{\mathbf{c}}^{\mathbf{I}}$ and $\boldsymbol{\sigma}_{\mathbf{d}}^{\mathbf{I}}$ are required for the determination of the four coefficients of the failure envelopes since numerical tests shows that equation (56) rewritten at microscopic scale for the epoxy matrix does not provide an additional relation between F_{1111}^m and F_{1122}^m:

$$F_{1122}^{m*} = \frac{F_{1122}^m}{\left|F_{1111}^m\right|} \neq -\frac{1}{2} \tag{58}$$

Moreover, according to (38-42) an uniaxial macroscopic tension or compression along the transverse (or normal) direction induces local mechanical states in the matrix generally exhibiting no zero strain and stress on-diagonal components (see for instance the cases of the macroscopic loads $\boldsymbol{\sigma}_{\mathbf{a}}^{\mathbf{I}}$ and $\boldsymbol{\sigma}_{\mathbf{b}}^{\mathbf{I}}$ on Table 7). As a consequence, only the strength coefficient F_{1212}^m can be determined independently from the three others, from the single macroscopic load $\boldsymbol{\sigma}_{\mathbf{d}}^{\mathbf{I}}$. Concerning the calculation of $F_{1111}^m, F_{1122}^m, F_{11}^m$, one has to solve numerically the system (60) (cf. Table 7).
Finally, the uniaxial microscopic ultimate stresses of the epoxy matrix embedded in the composite structure can be deduced from the set of equations (55) expressed at microscopic scale (i.e. replacing the subscripts ^{I} by the subscript ^{m}), provided that the coefficients of the local failure envelope are already known:

$$\begin{cases} X^m = Y^m = Z^m = \dfrac{1}{2\,F^m_{1111}}\left(\sqrt{F^{m\,2}_{11} + 4\,F^m_{1111}} - F^m_{11}\right) \\ X^{m'} = Y^{m'} = Z^{m'} = \dfrac{1}{2\,F^m_{1111}}\left(\sqrt{F^{m\,2}_{11} + 4\,F^m_{1111}} + F^m_{11}\right) \\ S^m = \dfrac{1}{\sqrt{2\,F^m_{1212}}} \end{cases} \tag{62}$$

The method, developed in the present paragraph, enables the determination of a) the coefficients of the microscopic failure envelope of the epoxy matrix in stress and/or strain space from the macroscopic failure envelope of the ply and scale transition relations linking macroscopic loads to the corresponding local microscopic mechanical states experienced by the matrix, only thereafter, b) the local maximum strength of the matrix embedding the carbon fibers which can be evaluated from the classical formalism relating the strength to the coefficients of the failure envelope. This inverse method provides an alternative to the classical direct approach leading to the determination of the failure envelope from the maximum strength measured on pure epoxies, in the cases that the required data is not available or when the behaviour of the matrix embedded in the composite structure is expected to be significantly different from the behaviour of the pure matrix, as shown for example, in references (Garett and Bailey, 1977; Christensen and Rinde, 1979).

5.3 Numerical applications and examples

5.4.1 Identification of the microscopic failure criteria of two typical epoxies from the knowledge of the macroscopic failure envelope of AS4/3501-6 and T300/N5208 composite plies

In the present paper, two types of high strength carbon fiber reinforced epoxies are considered: a) AS4/3501-6 and b) T300/N5208 composites having identical fiber volume fraction: v^f=0.6. These two materials constitute good candidates for the present work, since the microscopic strength of their respective matrix is not yet available (at our knowledge) in the already published literature, in spite of they are quite often considered for illustrating scientific works in this field of research (Tsai, 1987).
The macroscopic strength of single plies are given in Table 8. The coefficients of the corresponding quadratic macroscopic stress failure criteria, deduced from the classical direct method, through equation (55) are listed in Table 9.
In order to achieve the identification of the coefficients of the quadratic microscopic failure criteria of the pure epoxies (3501-6 and N5208, respectively), the method previously explained in subsection 5.2.3 was applied. The macroscopic stiffnesses considered for the simulation are provided in Table 10, whereas the elastic constants of the elastically isotropic resins, required for localising the macroscopic stress/strain states at the microscopic scale in the matrices, according to equations (38-42), were previously given in tables 1 and 5. In order to find the microscopic strength coefficients, four independent macroscopic stress states $\boldsymbol{\sigma}^{\mathbf{I}}_{\mathbf{a}}$, $\boldsymbol{\sigma}^{\mathbf{I}}_{\mathbf{b}}$, $\boldsymbol{\sigma}^{\mathbf{I}}_{\mathbf{c}}$, $\boldsymbol{\sigma}^{\mathbf{I}}_{\mathbf{d}}$ located on the macroscopic failure envelope according to the conditions described on the first raw of Table 7. Table 11 shows the strength coefficients found for the quadratic microscopic failure criterion in stress space of both epoxies by solving equations (60-61). Besides, the microscopic ultimate uniaxial stresses of the two studied epoxies have

been determined by introducing in equation (62) the results of the previous identification of the strength coefficients of their respective quadratic failure criterion in stress space (still Table 11). The corresponding results have been listed in Table 12.
Finally, instances of the microscopic failure envelopes have been drawn and superimposed to the corresponding macroscopic failure envelopes. Pictures of Figure 5 compare the results obtained in stress space for each couple epoxy/composite.

5.4.2 Observations on predicted results and discussion

According to the identification procedure described in subsection 5.2.3, an infinite number of macroscopic stress states sets $\{\boldsymbol{\sigma}_{\mathbf{a}}^{\mathbf{I}}, \boldsymbol{\sigma}_{\mathbf{b}}^{\mathbf{I}}, \boldsymbol{\sigma}_{\mathbf{c}}^{\mathbf{I}}, \boldsymbol{\sigma}_{\mathbf{d}}^{\mathbf{I}}\}$ can be considered for the determination of the researched microscopic failure envelope strength coefficients. Actually, $\boldsymbol{\sigma}_{\mathbf{c}}^{\mathbf{I}}$ only may vary whereas $\boldsymbol{\sigma}_{\mathbf{a}}^{\mathbf{I}}$, $\boldsymbol{\sigma}_{\mathbf{b}}^{\mathbf{I}}$ and $\boldsymbol{\sigma}_{\mathbf{d}}^{\mathbf{I}}$ are fixed by the macroscopic ultimate stresses Y^{I}, $Y^{I/}$, S^{I} of the considered composite structure (see the first raw of Table 7). Several tests were performed, introducing various numerical stress states (compatible with the constitutive hypotheses of the present work) for $\boldsymbol{\sigma}_{\mathbf{c}}^{\mathbf{I}}$. The tests showed that the microscopic strength coefficients are, as expected, independent from the choice of the initial macroscopic stress state $\boldsymbol{\sigma}_{\mathbf{c}}^{\mathbf{I}}$: one set of coefficients only is found as the unique solution of system (60). This demonstrates that the inverse model presented here is reliable from a numerical point of view.
The obtained results for the ultimate uniaxial stresses of 3501-6 and N5208 epoxies are close together (Table 12), whereas the macroscopic strength present significant discrepancies (Table 8). As an example, the relative deviation between the macroscopic longitudinal tensile ultimate stress of the two composites reaches around 25% when the relative deviation between the longitudinal tensile ultimate stress of the two epoxies is limited to 6%. Moreover, the representation of the microscopic failure envelopes are rather similar for the two considered resins, (Figure 5), whereas the macroscopic failure envelopes differ from one composite to the other (Figure 5, also). This could be interpreted as follows: for the considered composites, the observed deviation in the macroscopic failure envelopes comes from the choice of the reinforcing fibers and not from the choice of the resin. This is remarkable, since the considered epoxies exhibit a very different elastic mechanical behaviour (see Tables 1 and 5).
Moreover, the predicted microscopic ultimate uniaxial stresses are coherent with experimental results measured on plain resins. For instance, reference (Fiedler et al., 2001) reports a strength value of 117 MPa in compression, and elastic limits reaching respectively 29 MPa in tension and 31 MPa in torsion for small specimen of plain unreinforced Bisphenol-A type resin (i.e. “small” denotes a significantly reduced sized in normal and transverse directions compared to “bulk” specimen). These measured strength are of the same order of magnitude than the strength, calculated in the present work, for 3501-6 and N5208 epoxies. At the opposite, the strengths determined on bulk specimens of 5208 and 3501-6 plain epoxies are approximately two times higher than the values obtained in the present work, for the strength of the corresponding epoxies embedded in thin composite plies. This last result is also compatible with both the experimental comparison achieved in reference (Fiedler at al., 2001) on various sized pure epoxies and the practical comparisons of the failure mechanisms exhibited by composites structures and their constitutive epoxy resin (see Garett and Bailey, 1977; Christensen and Rinde, 1979). The present work allows to represent the scale effects observed in practice on the composite constituents strengths, because the composite ply strengths involved in the calculations do actually depend on both the constituents properties and microstructure.

6- Conclusions

The present work dealt with the question of scale transition modelling of polymer matrix composites and its application to several fields of investigation. Therefore, Mori-Tanaka and Eshelby-Kröner self-consistent models, taking advantage of arithmetic averages, were both considered for achieving the determinaiton of the homogenized properties of composite ply as a function of the properties of its constituents (on the one hand, the matrix , and on the second hand, the reinforcements).

The theoretical models properly take into account the specific microstructure of such materials. Especially the extreme morphology of the reinforcements can be considered, while the morphology and orientation of the reinforcing inclusions are kept constant in a single ply. As a consequence, the models manage to reproduce realistically the strong macroscopic anisotropy observed in practice on uni-directionally fiber-reinforced epoxies. The obtained results have shown that the two approaches, presented here, yield close together estimations of the macroscopic coefficients of thermal expansion, coefficients of moisture expansion and elastic moduli, in the range of the epoxy volume fraction, that is typical for designing composites structures for engineering applications $\left(\text{i.e. } 0.3 \le v^m \le 0.7\right)$. Nevertheless, an exception to this statement occurs for Coulomb modulus G_{12}^{I}, that is strongly underestimated in the case that the calculations are performed according to Mori-Tanaka approximation, in the same range of epoxy volume fractions.

Moreover, realistic inverse scale transition procedures based on Kröner-Eshelby self-consistent model and Mori-Tanaka estimates were also provided for achieving the numerical determination of the mechanical, hygroscopic or thermal properties of one constituent of an uni-directionally reinforced composite ply. Both models were used in order to estimate the elastic stiffness of reinforcing fibers embedded in a composite ply, from the knowledge of the macroscopic properties and those of the matrix. The obtained numerical results were successfully compared with expected practical results. A similar study was achieved in the standpoint of estimating the coefficients of moisture expansion of the matrix constituting a composite ply. In both cases the proposed theoretical approaches led to similar results, which is satisfying. Thus, the two inverse models described in the present work can be equally used in order to achieve such an identification.

Another section of this article was devoted to the analysis of the macroscopic mechanical states localization within the constituents of a composite ply. Since it was previously demonstrated in the literature, that Mori-Tanaka approximation was not reliable for handling such a task, only Eshelby-Kröner model was considered. A numerical model, valid for any morphology of the reinforcing inclusions, was provided. Moreover a rigorous fully analytical treatment of the classical Kröner and Eshelby Self-Consistent model including morphology effects was achieved also. Especially, the determination of Morris' tensor was performed in a satisfactory agreement with the transverse macroscopic elastic anisotropy expected for the fiber shape that should be taken into account in order to satisfactory represent the specific microstructure of carbon-fiber reinforced composites. The new closed-form solutions obtained for the components of Morris' tensor were introduced in the classical hygro-thermo-elastic scale transition relation in order to express analytically the internal strains and stresses in both the fiber and the resin of a ply submitted to a hygro-thermo-elastic load. The closed-form solution demonstrated in the present work was compared to the fully numerical self-consistent model for various geometrical arrangements of the fibers: uni-directional or laminated composites. A very good agreement was obtained between the two models for any component of the local stress tensors. It was also demonstrated that continuum mechanics and

micro-mechanical models give complementary information about the occurrence of a possible damage during the loading of the structure.
In a last part, the present study explained a procedure enabling to achieve the identification of one single set of strength parameters defining completely the microscopic failure envelope of the matrix entering in the composition of a composite structure, in the cases that a pure mechanical load is applied. The identification method was built around an inverse scale transition method which requires the knowledge of the macroscopic strengths, and both the macroscopic and microscopic elastic stiffnesses. Besides, it was necessary to consider some hypotheses in order to proceed to the identification of the coefficients of the microscopic quadratic failure criteria. In the present work, it was assumed that the macroscopic failure of a uni-directionally reinforced ply is dominated by the local failure of the matrix when the external load is applied in planes perpendicular to the fiber axis.
Numerical applications of the proposed inverse method were made considering the cases of two high-strength composites structures: AS4/3501-6 and T300/N5208. The determination of the microscopic quadratic failure criterion of the pure epoxies (3501-6 and N5208, respectively) was achieved. The obtained results are close together and present a good agreement with ultimate strengths measured on reduced sized plain resins (available from already published literature). This demonstrates the reliability of the present predictive method for estimating the local failure behaviour of epoxies whose experimental failure criterion has not yet been determined.
In further works, the proposed approach will be extended to the more general case of hygro-thermo-mechanical loads. This will imply to take into account the stress free strains in order to keep consistency between the failure envelopes expressed in stress and strain spaces. Besides, the rigorous treatment of the hygro-thermo-mechanical load requires to consider the dependence on the temperature and moisture content of a) the elastic stiffness, coefficients of thermal expansion and coefficients of moisture expansion and b) the ultimate strength (and in general, the coefficients of the considered failure criterion), at both macroscopic and microscopic scales. Others perspectives of research are proposed in the following section below.

7- Perspectives

Scale transition modelling based theoretical analysis of composite structures constitutes an overexpanding field of research, due to multiple factors. Among them, the emergence of new materials exhibiting a specific, more advanced microstructure, the ambition to account for additional, sometimes only recently discovered, physical phenomena and the relentless research for building faster, more convenient but still reliable models stand for the three essential motivations for achieving further developments in the incoming years.

7.1 Emergence of new materials

The present development stage of Eshelby's single inclusion theory involved in the mechanical modeling of composites is not intended for a rigorous treatment of the morphology presented by the reinforcements used for manufacturing woven-composites. As a consequence, answering to the question of a theoretical study, through scale transition models, of mechanical parts made of such composites will require a specific and still missing solution.
Since the recent discovery of carbon nanotubes in the 90's, researchers worldwide have engaged in fundamental studies of this novel material (Treacy et al., 1996). The pioneering works have underlined the characteristics of carbon nanotubes such as an extraordinarily high stiffness (Salvetat et al., 1999) coupled to a high tensile strength (Demczyk et al., 2002)., high

aspect ratio and an especially low density. Actually, for instance, the experimental direct mechanical measurement of the elastic properties of carbon nanotubes provided Young's moduli in the range of 1 TPa, which considerably exceeds the corresponding modulus of any currently available fiber material (Salvetat et al., 1999; Demczyk et al., 2002).
In consequence, the technological applications of carbon nanotubes as reinforcements for elastomers (Frogley et al., 2003) or polymer-based composites (Liu and Wagner, 2005; Breton et al., 2004; Xiao et al., 2006) was very recently investigated. Furthermore, multi-materials made up of polymer matrix, carbon fibers and carbon nanotubes are considered also for achieving a new generation of engineering composites.

7.2 Accounting for additional physical factors

The present work is focused on the theoretical prediction of the mechanical behaviour of composite structures submitted also to environmental conditions. However, every aspect of the consequences of environmental loading on the constituents of composite materials have not always been considered in this paper, for the sake of simplicity. Nevertheless, accounting for some additional physical factors would improve the realism and the reliability of the predictions obtained through the scale-transition models.
For instance, the moisture diffusion process was assumed, in the present work, to follow the linear, classical, established for a long time, Fickian model. Nevertheless, some valuable experimental results, already reported in (Gillat and Broutman, 1978), have shown that certain anomalies in the moisture sorption process, (i.e. discrepancies from the expected Fickian behaviour) could be explained from basic principles of irreversible thermodynamics, by a strong coupling between the moisture transport in polymers and the local stress state (Weitsman, 1990a, Weitsman, 1990b).
The present work yields several perspectives of research concerning the application of scale transition model to the identification of composite materials properties. Moisture and temperature are not the only parameters leading to an evolution of the mechanical properties of epoxies. According to the literature, thermo-oxidation is reported to enhance the stiffness of the epoxies (Decelle et al., 2003 ; Ho and al., 2006). The inverse methods presented here could for instance be directly applied to the estimation of the epoxy stiffening from the knowledge of the macroscopic elastic properties evolution as a function of the mass loss during the thermo-oxidation process. Furthermore, extensions of the inverse models could be achieved in order to account for the variation of the coefficients of thermal and/or moisture expansion of the constituents of a composite ply, enabling to identify them and their evolutions as a function of the environmental conditions. Finally, a similar approach could be developed in order to identify the damage induced evolution of the mechanical behaviour of the constituents of composite plies from the inelastic part of macroscopic stress/strain curves. The experimental data required for achieving such analysis is already available in the literature (Soden et al., 1998). Nevertheless, local and macroscopic damage have still to be implemented in the theoretical laws. The above-listed perspectives of research will be successively considered in further works.

7.3 Improving the calculation time while ensuring the most reliable predictions

The present work underlines the sometime existing opportunity to replace purely numerical mathematical solutions by analytical forms enabling to significantly reduce both the time required for designing the software and the time necessary for achieving one simulation. It was demonstrated in this paper that Eshelby-Kröner could be, at least partially, presented as an analytical model, while it was used for predicting mechanical states. Nevertheless, the

estimation of the macroscopic properties (elastic stiffness, coefficients of thermal expansion and coefficients of moisture expansion) through the homogenization relations deduced from this very model do still involve an implicit iterative procedure. It was already shown in the literature by Welzel and his co-authors, that under specific conditions, it was possible to build a model, numerically equivalent to Eshelby-Kröner model, from the combination of two (separately less successful) other models (Welzel, 2002 ; Welzel et al. 2003). The concept is similar to the idea based on empirical comparisons, historically proposed by Neerfeld (Neerfeld, 1942) and Hill (Hill, 1952) to average Reuss and Voigt rough hypotheses in order to get a numerically acceptable theoretical solution. In the field of micro-mechanical modelling of composite materials, a combination of the two possible localization procedures considered for Mori-Tanaka model in the present work would enable to numerically reproduce the homogenized properties obtained from Eshelby-Kröner model. Building an effective model from the two main ways of writing Mori-Tanaka model would mainly enable to obtain closed-form solutions for the elastic stiffness tensor, instead of having to numerically solve the iterative procedure involved in Eshelby-Kröner self-consistent model. Thus, a coupling of this numerically effective solution for predicting realistic hygrothermo-mechanical macroscopic properties to the already proposed in this very article analytical forms for the local mechanical states would yield to a faster but still extremely reliable innovative scale-transition approach for studying composite materials. The analytical forms required for achieving the effective Mori-Tanaka model should be derived and published in the near future.

References

Agbossou, A., Pastor J. (1997). Thermal stresses and thermal expansion coefficients of n-layered fiber-reinforced composites, *Composites Science and Technology*, **57**: 249-260.

Asaro, R. J. and Barnett, D. M. (1975). The non-uniform transformation strain problem for an anisotropic ellipsoidal inclusion, *Journal of the Mechanics and Physics of Solid*s, **23**: 77-83.

Baptiste, D. (1996). Evolution des contraintes dans les matériaux composites – Modélisation micromécanique du comportement des composites à renforts discontinus, In: *Analyse des contraintes résiduelles par diffraction des rayons X et des neutrons*, Alain Lodini and Michel Perrin (Editors).

Benveniste, Y. (1987). A New Approach to the Application of Mori-Tanaka's Theory in Composite Materials, *Mechanics of Materials*, **6**: 147-157.

Bowles, D.E., Post, D., Herakovich, C.T., and Tenney, D.R. (1981). Moiré Interferometry for Thermal Expansion of Composites, *Exp. Mech.*, **21**: 441-447.

Breton, Y., Désarmot, G., Salvetat, J.P., Delpeux, S., Sinturel, C., Béguin, F. et Bonnamy, S. (2004). Mechanical properties of multiwall carbon nanotubes/epoxy composites : influence of network morphology, *Carbon*, **42**: 1027-1030.

Christensen, R. M. and Rinde, J. A. (1979). Transverse tensile characteristics of fiber composites with flexible resins : theory and test results, *Pol. Eng. Sci.*, **19**: 506-511.

Crank, J. (1975). *The mathematics of diffusion*, Clarendon Press, Oxford.

Cuntze, R. G. (2003). The predictive capability of failure mode concept-based strength criteria for multi-directional laminates – part B, *Composite Science and Technology*, **64**: 487-516.

Daniel, I. M., and Ishai, O. (1994). In: "Engineering Mechanics of Composite Materials", Oxford University Press.

Decelle, J., Huet, N. and Bellenger, V. (2003). Oxidation induced shrinkage for thermally aged epoxy networks, *Polymer Degradation and Stability*, **81**: 239-248.

Demczyk, B.G., Wang, Y.M., Cumings, J., Hetman, M., Han, W., Zettl, A., and Ritchie, R. O. (2002). « Direct mechanical measurement of the tensile strength and elastic modulus of multiwalled carbon nanotubes », *Mat. Sci. Eng.*, **A334**: 173-178.

DiCarlo, J.A. (1986). Creep of chemically vapor deposited SiC fiber, *J. Mater. Sci.*, **21**: 217-224.

Dyer, S.R.A., Lord, D., Hutchinson, I.J., Ward, I.M. and Duckett, R.A. (1992). Elastic anisotropy in unidirectional fibre reinforced composites, *J. Phys. D: Appl. Phys.*, **25**: 66-73.

Eshelby, J. D. (1957). The Determination of the Elastic Field of an Ellipsoidal Inclusion, and Related Problems, In: *Proceedings of the Royal Society London*, **A241**: 376–396.

Ferreira, C., Casari, P., Bouzidi, R. and Jacquemin, F. (2006a). Identification of Young Modulus Profile in PVC Foam Core thickness using speckle interferometry and Inverse Method, *Proceedings of SPIE - The International Society for Optical Engineering*.

Ferreira, C., Jacquemin, F. and Casari, P. (2006b). Measurement of the nonuniform thermal expansion coefficient of a PVC foam core by speckle interferometry - Influence on the mechanical behavior of sandwich structures, *Journal of Cellular Plastics*, **42** (5): 393-404.

Fiedler, B., Hojo, M., Ochiai, S., Schulte, K. and Ando, M. (2001), Failure behaviour of an epoxy matrix under different kinds of static loading, *Composite Science and Technology*, **61**: 1615-1624.

Fleck, N. A. and Jelf, P. M. (1995). Deformation and failure of a carbon fibre composite under combined shear and transverse loading, *Acta metall. mater.*, **43**: 3001-3007.

François, M. (1991). Détermination de contraintes résiduelles sur des fils d'acier eutectoïde de faible diamètre par diffraction des rayons X, Doctoral Thesis, ENSAM, Paris.

Fréour, S., Gloaguen, D., François, M., Guillén, R., Girard, E. and Bouillo, J. (2002) Determination of the macroscopic elastic constants of a phase embedded in a multiphase polycrystal – application to the beta-phase of Ti17 titanium based alloy, *Materials Science Forum*, **404-407**: 723-728.

Fréour, S., Gloaguen, D., François, M. and Guillén, R. (2003a). Study of the Coefficients of Thermal Expansion of Phases Embedded in Multiphase Materials, *Material Science Forum*, **426–432**: 2083–2088.

Fréour, S., Gloaguen, D., François, M. and Guillén, R. (2003b). Thermal properties of polycrystals - X-ray diffraction and scale transition modelling, *Physica Status Solidi a*, **201**: 59-71.

Fréour, S., Jacquemin, F. and Guillén, R. (2005a). On an analytical Self-Consistent model for internal stress prediction in fiber-reinforced composites submitted to hygro-elastic load, *Journal of Reinforced Plastics and Composites*, **24**: 1365-1377.

Fréour, S., Gloaguen, D., François, M., Perronnet, A. and Guillén, R. (2005b). Estimation of Ti-17 β–phase Single-Crystal Elasticity Constants using X-Ray Diffraction measurements and inverse scale transition modelling, *Journal of Applied Crystallography*, **38**: 30-37.

Fréour, S., Jacquemin, F. and Guillén, R. (2006a). Extension of Mori-Tanaka Approach to Hygroelastic Loading of Fiber-Reinforced Composites – Comparison with Eshelby-Kröner Self-consistent Model, *Journal of Reinforced Plastics and Composites*, **25**: 1039-1052.

Fréour, S., Gloaguen, D., François, M. and Guillén, R. (2006b). Application of inverse models and XRD analysis to the determination of Ti-17 β–phase Coefficients of Thermal Expansion, *Scripta Materialia*, **54**: 1475-1478.

Fréour, S., Jacquemin, F. and Guillén, R. (to be published). On the use of the geometric mean approximation in estimating the effective hygro-elastic behaviour of fiber-reinforced composites, *Journal of Materials Science.*

Frogley, M.D., D. Ravich, D., and Wagner, H.D. (2003). "Mechanical properties of carbon nanoparticle-reinforced elastomers", *Comp. Sci. Tech.*, **63**: 1647-1654.

Garett, K. W. and Bailey, J. E. (1977). The effect of resin failure strain on the tensile properties of glass fiber-reinforced polyester cross-ply laminates, *J. Mater. Sci.*, **12**: 2189-2194.

Gillat, O. and Broutman, L.J. (1978). "Effect of External Stress on Moisture Diffusion and Degradation in a Graphite Reinforced Epoxy Laminate", *ASTM STP*, **658**: 61-83.

Gloaguen, D., François, M., Guillén, R. and Royer, J. (2002). Evolution of Internal Stresses in Rolled Zr702, *Acta Materialia*, **50**: 871–880.

Han, J., Bertram, A., Olschewski, J., Hermann, W. and Sockel, H.G. (1995). Identification of elastic constants of alloys with sheet and fibre textures based on resonance measurements and finite element analysis. *Materials Science and Engineering*, **A191**: 105-111.

Herakovitch, C. T. (1998). *Mechanics of Fibrous Composites*, John Wiley and Sons Inc., New York.

Hill, R. (1952). The elastic behaviour of a crystalline aggregate. *Proc. Phys. Soc.*, **65**: 349-354.

Hill, R., (1965). Continuum micro-mechanics of elastoplastic polycrystals, *J. Mech. Phys. Solids*, **13**: 89-101.

Hill, R. (1967). The essential structure of constitutive laws for metals composites and polycrystals, *Journal of the Mechanics and Physics of Solids*, **15**: 79-95.

Ho, N.Q., Pons, F. and Lafarie-Frenot, M.C. (2006). Characterization of an Oxidized Layer in Epoxy Resin and in Carbon Epoxy Composite for Aeronautic Applications, *Proceedings of ECCM 12*.

Jacquemin, F. and Vautrin, A. (2002). A Closed-form Solution for the Internal Stresses in Thick Composite Cylinders Induced by Cyclical Environmental Conditions, *Composite Structures*, **58**: 1–9.

Jacquemin, F., Fréour, S., and Guillén, R. (2005). A self-consistent approach for transient hygroscopic stresses and moisture expansion coefficients of fiber-reinforced composites, *Journal of Reinforced Plastics and Composites*, **24**: 485-502.

Kaddour, A. S., Hinton, M. J. and Soden, P. D. (2003). Behaviour of ± 45° glass/epoxy filament wound composite tubes under quasi-static equal biaxial tension-compression loading: experimental results, *Composites : part B*, **34**: 689-704.

Karakazu, R., Atas, C. and Akbulut, H. (2001). Elastic-plastic Behaviour of Woven-steel-fiber-reinforced Thermoplastic Laminated Plates under In-plane Loading, *Composites Science and Technology*, **61**: 1475-1483.

Khashaba, U. A., (2004). In-plane shear properties of cross-ply composite laminates with different off-axis angles, Composite Structures, **65**: 167-177.

Kocks, U. F., Tomé , C. N. and Wenk, H. R. (1998). Texture and Anisotropy, Cambridge University Press.

Kröner E. (1953). *Dissertation*, Technischen Hochschule Stuttgart.

Kröner, E. (1958). "Berechnung der elastischen Konstanten des Vielkristalls aus des Konstanten des Einkristalls", *Zeitschrift für Physik*, **151**: 504–518.

Liu, K-S and Tsai, S. W. (1998). A progressive quadratic failure criterion for a laminate, *Composite Science and Technology*, **58**: 1023-1032.

Liu, L. et Wagner, H.D. (2005). Rubery and gassy epoxy resins reinforced with carbon nanotubes, *Comp. Sci. Tech.*, **65**: 1865-1868.

Loos, A. C. and Springer, G. S. (1981). Environmental Effects on Composite Materials, Moisture Absorption of Graphite – Epoxy Composition Immersed in Liquids and in Humid Air, pp. 34–55, Technomic Publishing.

Mabelly, P. (1996). Contribution à l'étude des pics de diffraction – Approche expérimentale et modélisation micromécanique, Doctoral Thesis, ENSAM, Aix en Provence.

Matthies, S., and Humbert, M. (1993). The realization of the concept of a geometric mean for calculating physical constants of polycrystalline materials, *Phys. Stat. Sol. b*, **177**: K47-K50.

Matthies, S., Humbert, M., and Schuman, Ch. (1994). On the use of the geometric mean approximation in residual stress analysis", *Phys. Stat. Sol. b*, **186** : K41-K44.

Matthies, S. Merkel, S., Wenk, H.R., Hemley, R.J. and Mao, H. (2001). Effects of texture on the determination of elasticity of polycrystalline ε-iron from diffraction measurements, Earth and Planetary Science Letters, **194**: 201-212.

Mensitieri, G. M., Del Nobile, M. A., Apicella, A. and Nicolais, L. (1995). Moisture-matrix interactions in polymer based composite materials, *Revue de l'Institut Français du Pétrole*, **50**: 551-571.

Morawiec, A. (1989). Calculation of polycrystal elastic constants from single-crystal data, *Phys. Stat. Sol. b*, **154** : 535-541.

Mori, T. and Tanaka, K. (1973). Average Stress in Matrix and Average Elastic Energy of Materials with Misfitting Inclusions, *Acta Metallurgica,* **21**: 571-574.

Morris, R. (1970). Elastic constants of polycrystals, *Int. J. Eng. Sci.*, **8**: 49.

Mura, T. (1982). *Micromechanics of Defects in Solids*, Martinus Nijhoff Publishers, The Hague, Netherlands.

Neerfeld, H. (1942). Zur Spannungsberechnung aus röntgenographischen Dehnungsmessungen, *Mitt. Kaiser-Wilhelm-Inst. Eisenforschung Düsseldorf* **24**: 61-70.

Qiu, Y. P. and Weng, G. J. (1991). The influence of inclusion shape on the overall elastoplastic behavior of a two-phase isotropic composite, *Int. J. Solids Structures*, **27** (12): 1537-1550.

Reuss, A. (1929). Berechnung der Fliessgrenze von Mischkristallen auf Grund der Plastizitätsbedingung für Einkristalle, *Zeitschrift für Angewandte und Mathematik und Mechanik*, **9**: 49–58.

Sai Ram K.S., Sinha, P.K. (1991). Hygrothermal effects on the bending characterics of laminated composite plates, *Computational Structure,* **40** (4): 1009-1015.

Salvetat, J.-P., Andrews, G., Briggs, D., Bonard, J.-M., Bacsa, R.R., Kulik, A.J., Stöckli, T., Burnham, N.A., and Forro, L. (1999). "Elastic and Shear Moduli of Single-Walled Carbon Nanotube Ropes", *Phys. Rev. Lett.*, **82**: 944-947.

Sims, G.D., Dean, G.D., Read, B.E. and Western B.C. (1977). Assessment of Damage in GRP Laminates by Stress Wave Emission and Dynamic Mechanical Measurements, *Journal of Materials Science,* **12** (11): 2329-2342.

Soden, P. D., Hinton M. J. and A. S. Kaddour, A. S. (1998). Lamina properties lay-up configurations and loading conditions for a range of fiber-reinforced composite laminates, *Composites Science and Technology*, **58**: 1011-1022.

Sprauel, J. M., and Castex, L. (1991). First European Powder Diffraction International Conference on X-Ray stress analysis, Munich.

Tanaka, K. and Mori, T. (1970). The Hardening of Crystals by Non-deforming Particules and Fibers, *Acta Metallurgica*, **18**: 931-941.

Treacy, M.M.J., Ebbesen, T.W. and Gibson, T.M. (1996). "Exceptionally high Young's modulus observed for individual carbon nanotubes", *Nature*, **381**: 678-680.

Tsai, C.L. and Daniel I.M. (1993). Measurement of longitudinal shear modulus of single fibers by means of a torsional pendulum. 38th International SAMPE Symposium 1993:1861-1868.

Tsai C.L. and Daniel I.M. (1994). Method for thermo-mechanical characterization of single fibers, *Composites Science and Technology*, **50**: 7-12.

Tsai, C.L. and Chiang, C.H. (2000). Characterization of the hygric behavior of single fibers. *Composites Science and Technology*, **60**: 2725-2729

Tsai, S. W. and Hahn, H. T. (1980). *Introduction to composite materials*, Technomic Publishing Co., Inc., Lancaster, Pennsylvania.

Tsai, S. W. (1987). Composite Design, 3rd edn, Think Composites.

Turner, P. A. and Tome, C. N. (1994). "A Study of Residual Stresses in Zircaloy-2 with Rod Texture", *Acta Metallurgica and Materialia*, **42**: 4143–4153.

Voigt, W. (1928). Lehrbuch der Kristallphysik, Teubner, Leipzig/Berlin.

Weitsman, Y. (1990a). "A Continuum Diffusion Model for Viscoelastic Materials", *Journal of Physical Chemistry*, **94**: 961-968.

Weitsman, Y. (1990b). "Moisture in Composites: Sorption and Damage", in: Fatigue of Composite Materials. Elsevier Science Publisher, K.L. Reifsnider (editor), 385-429.

Welzel, U. (2002). "Diffraction Analysis of Residual Stress; Modelling Elastic Grain Interaction.", PhD thesis, University of Stuttgart, Germany.

Welzel, U., Leoni, M. and Mittemeijer, E. J. (2003). « The determination of stresses in thin films; modelling elastic grain interaction », *Philosophical Magazine*, **83**: 603-630.

Welzel, U., Fréour, S. and Mittemeijer, E. J. (2005). « Direction-dependent elastic grain-interaction models – a comparative study », *Philosophical Magazine*, **85**: 2391-2414.

Xiao, K.Q., Zhang, L.C. et Zarudi, I. (2006). « Mechanical and rheological properties of carbon nanotube-reinforced polyethylene composites », *Comp. Sci. Tech.*, **67**: 177-182.

Figure captions

Figure 1: Macroscopic effective hygro-thermo-mechanical properties of T300/N5208 plies, estimated as a function of the epoxy volume fraction, through scale transition homogenization procedures. Comparison between Mori-Tanaka approximate and Kröner-Eshelby self-consistent model.

Figure 2: Time dependent concentration profiles in T300/5208 as a function of the normalised radial distance from the inner radius r_{dim}.

Figure 3: Local stresses in T300/5208 composite for the central ply, in the case of a) the uni-directionaly reinforced composite and b) the $[+55°/-55°]_S$ symmetric laminate. CMF stands for Continuum Mechanics Formalisms.

Figure 4: Local stresses in T300/5208 composite for the inner ply, in the case of a) the uni-directionaly reinforced composite and b) the $[+55°/-55°]_S$ symmetric laminate. CMF stands for Continuum Mechanics Formalisms.

Figure 5: Examples of macroscopic and local (matrix only) stress failure envelopes of T300/5208 and AS4/3501-6 plies.

Table captions

Table 1: Hygro-thermo-mechanical properties of T300/5208 constituents.

Table 2: Macroscopic elastic moduli (from the literature) and stiffness tensor components (calculated) considered for the composite ply at $\Delta C^I = 0$ % and T^I = 300 K, according to (Sai Ram and Sinha, 1991).

Table 3: Pseudomacroscopic elastic moduli and stiffness tensor components assumed for the epoxy matrix of the composite plies at $\Delta C^I = 0$ % and T^I = 300 K, according to (Herakovich, 1998).

Table 4: Pseudomacroscopic elastic moduli and stiffness tensor components identified for the carbon fiber reinforcing the composite plies at $\Delta C^I = 0$ % and T^I = 300 K, according to either Mori-Tanaka estimates, or Eshelby-Kröner self-consistent model. Comparison with the corresponding properties exhibited in practice by typical high-strength carbon fibers, according to (Herakovich, 1998).

Table 5: Macroscopic and pseudo-macroscopic mechanical elastic properties of AS4/3501-6 constituents.

Table 6: Macroscopic and pseudomacroscopic (3501-6 matrix only) coefficients of moisture expansion of AS4/3501-6 composite. The pseudomacroscopic values results from the two inverse scale transition models described in the present work.

Table 7: one possible set of trials enabling the determination of the microscopic strength coefficients of the matrix expressed in stress space.

Table 8: macroscopic strength data.

Table 9: quadratic macroscopic stress failure criteria deduced from the strength data. Quadratic *ijkl* subscripted coefficients [MPa^{-2}] and linear *ij* subscripted coefficients [MPa^{-1}].

Table 10: macroscopic stiffness components [GPa] of 60% volume uni-directionally fiber reinforced plies. Fiber axis is parallel to longitudinal direction.

Table 11: quadratic local stress failure criteria in N5208 and 3501-6 epoxy matrices respectively deduced from the macroscopic failure envelopes of T300/5208 and AS4/3501-6 plies, taking into account the microscopic elastic properties given on tables 1 and 5. Quadratic *ijkl* subscripted coefficients [MPa^{-2}] and linear *ij* subscripted coefficients [MPa^{-1}].

Table 12: local (matrix embedded in a composite ply) strength data deduced from the local quadratic stress failure criteria of a N5208 and 3501-6 epoxy matrices respectively.

Figures

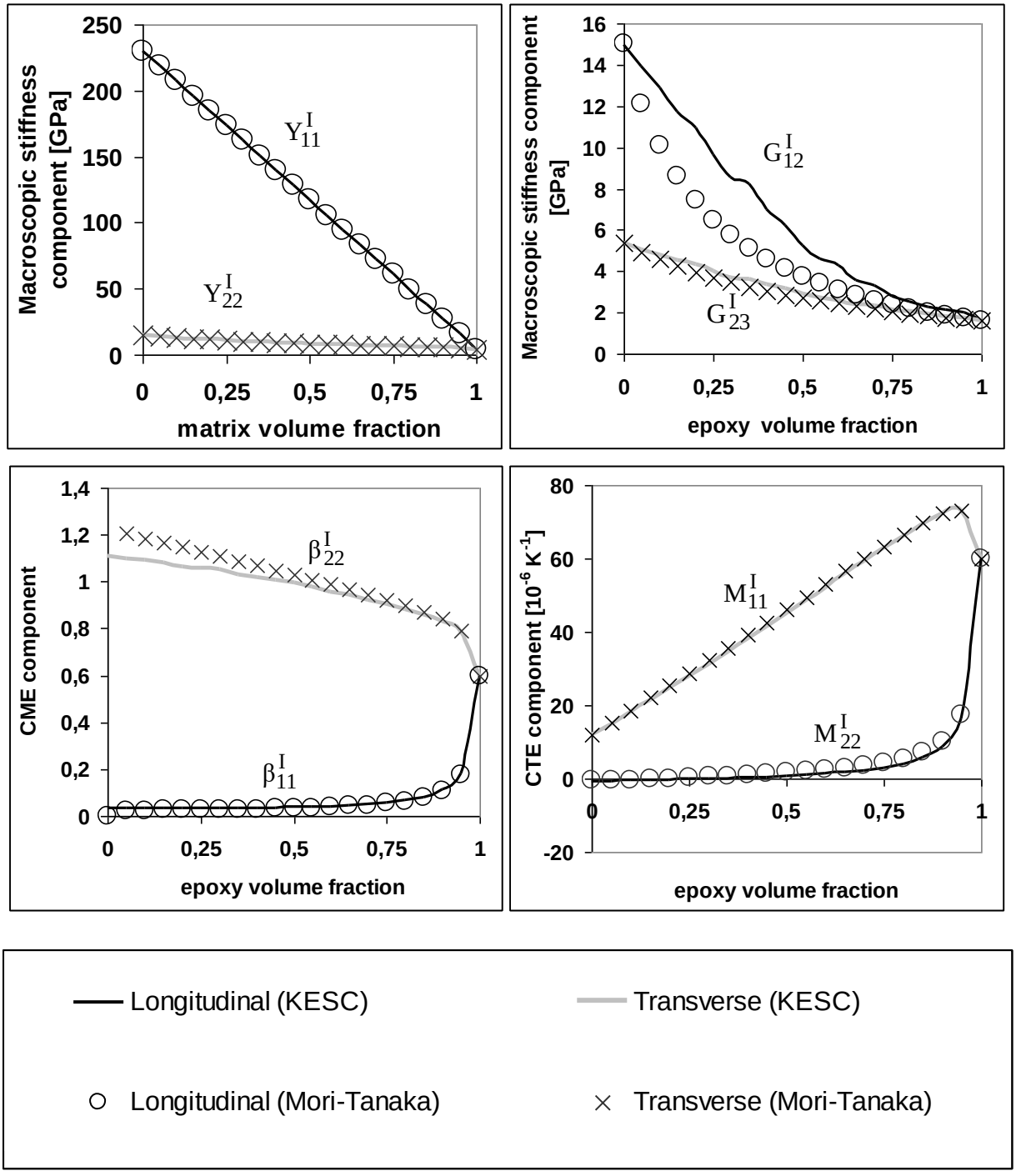

Figure 1: Macroscopic effective hygro-thermo-mechanical properties of T300/N5208 plies, estimated as a function of the epoxy volume fraction, through scale transition homogenisation procedures. Comparison between Mori-Tanaka approximate and Kröner-Eshelby self-consistent model.

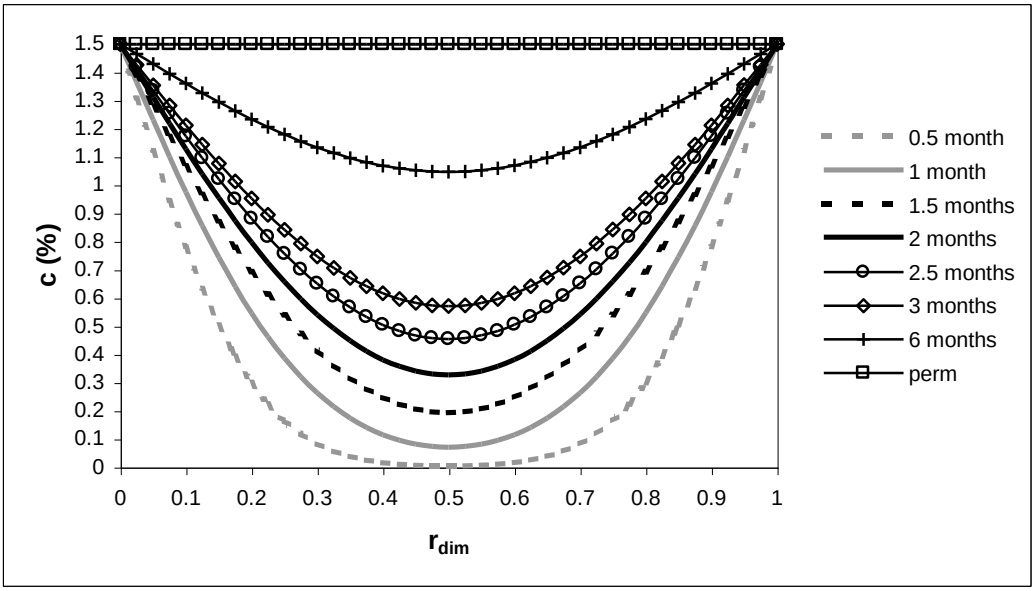

Figure 2: Time dependent concentration profiles in T300/5208 as a function of the normalised radial distance from the inner radius r_{dim}.

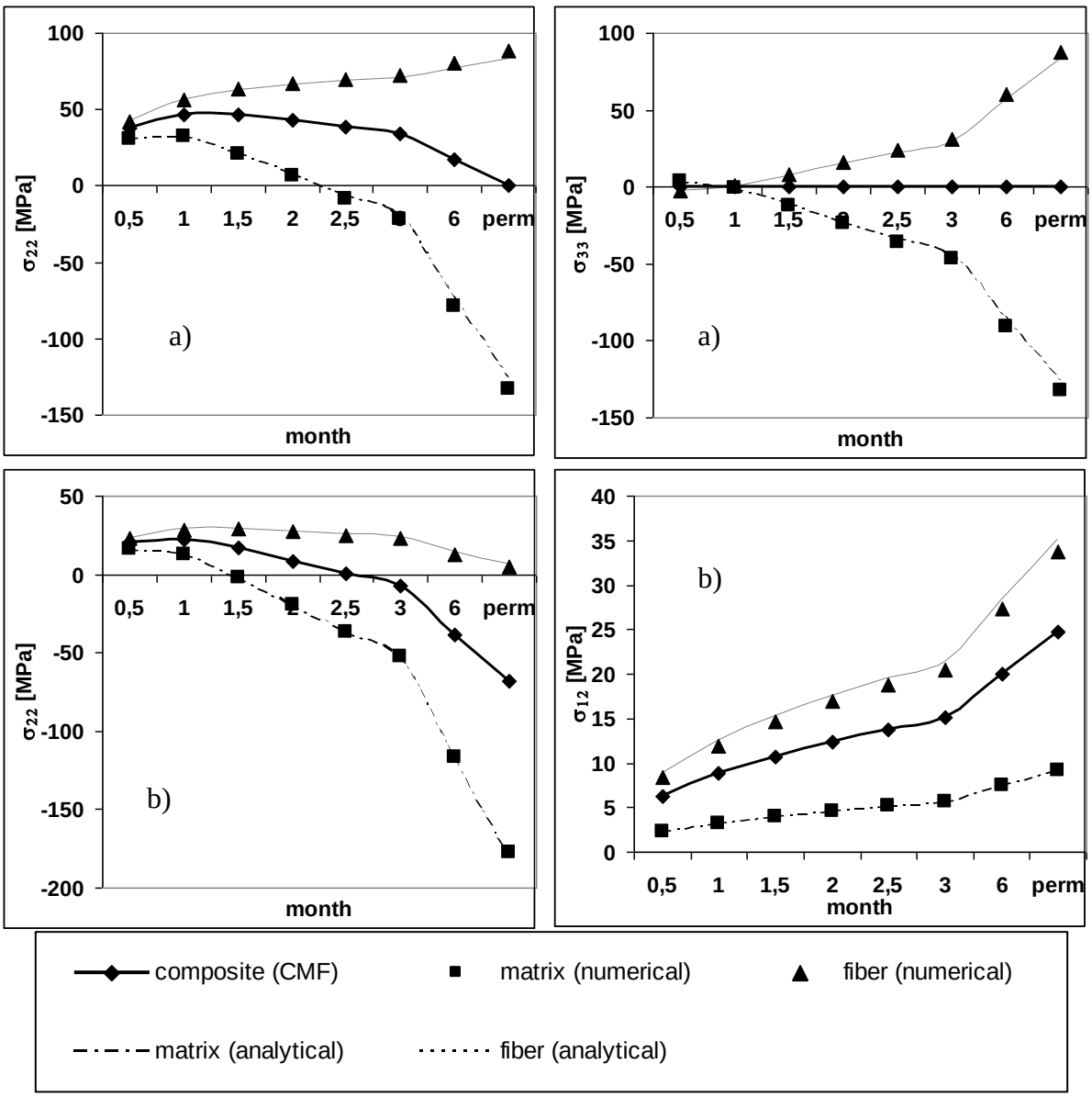

Figure 3: Local stresses in T300/5208 composite for the central ply, in the case of a) the uni-directionaly reinforced composite and b) the $[+55°/-55°]_S$ symmetric laminate. CMF stands for Continuum Mechanics Formalisms.

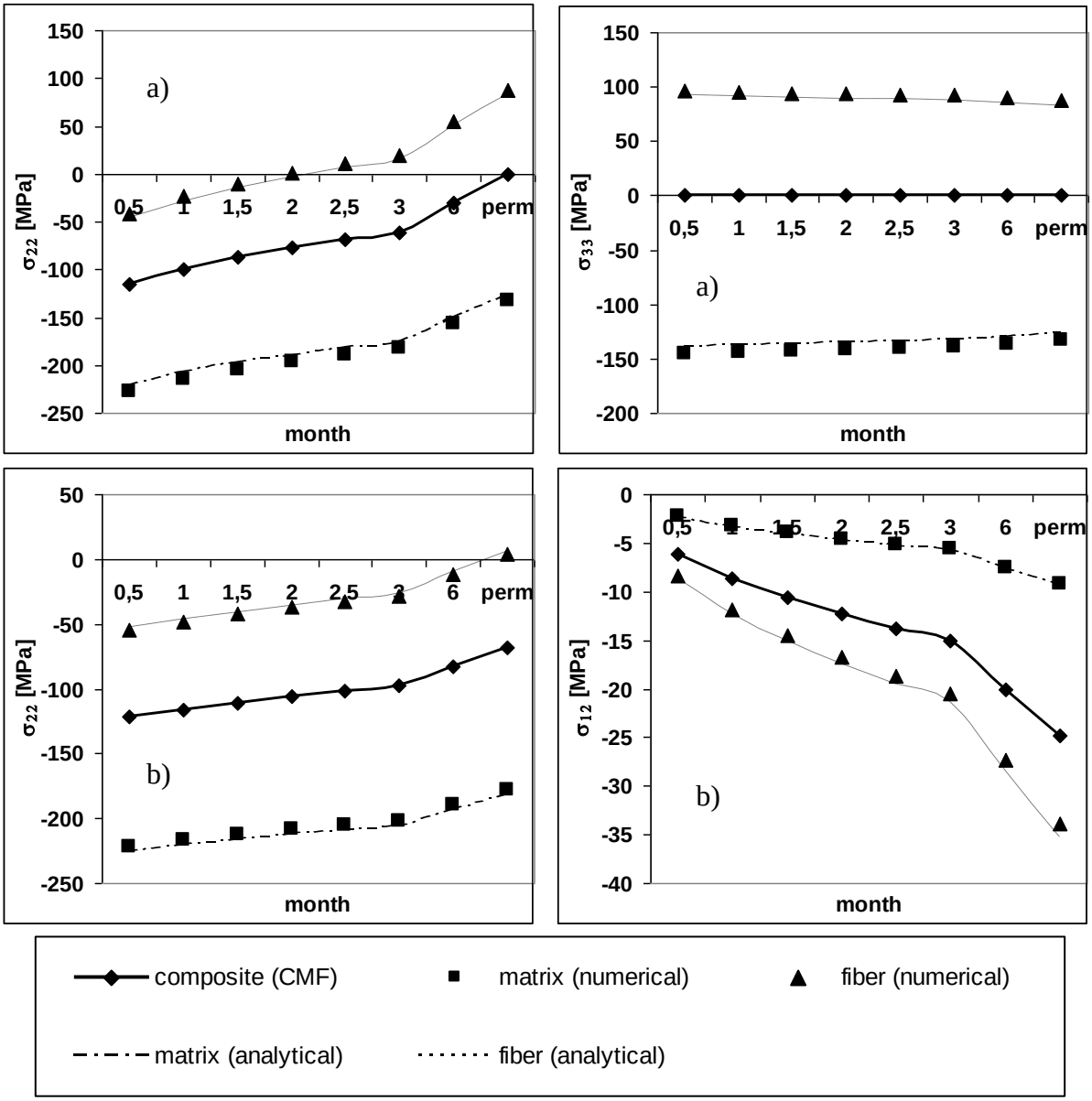

Figure 4: Local stresses in T300/5208 composite for the inner ply, in the case of a) the uni-directionaly reinforced composite and b) the [+55°/-55°]s symmetric laminate. CMF stands for Continuum Mechanics Formalisms.

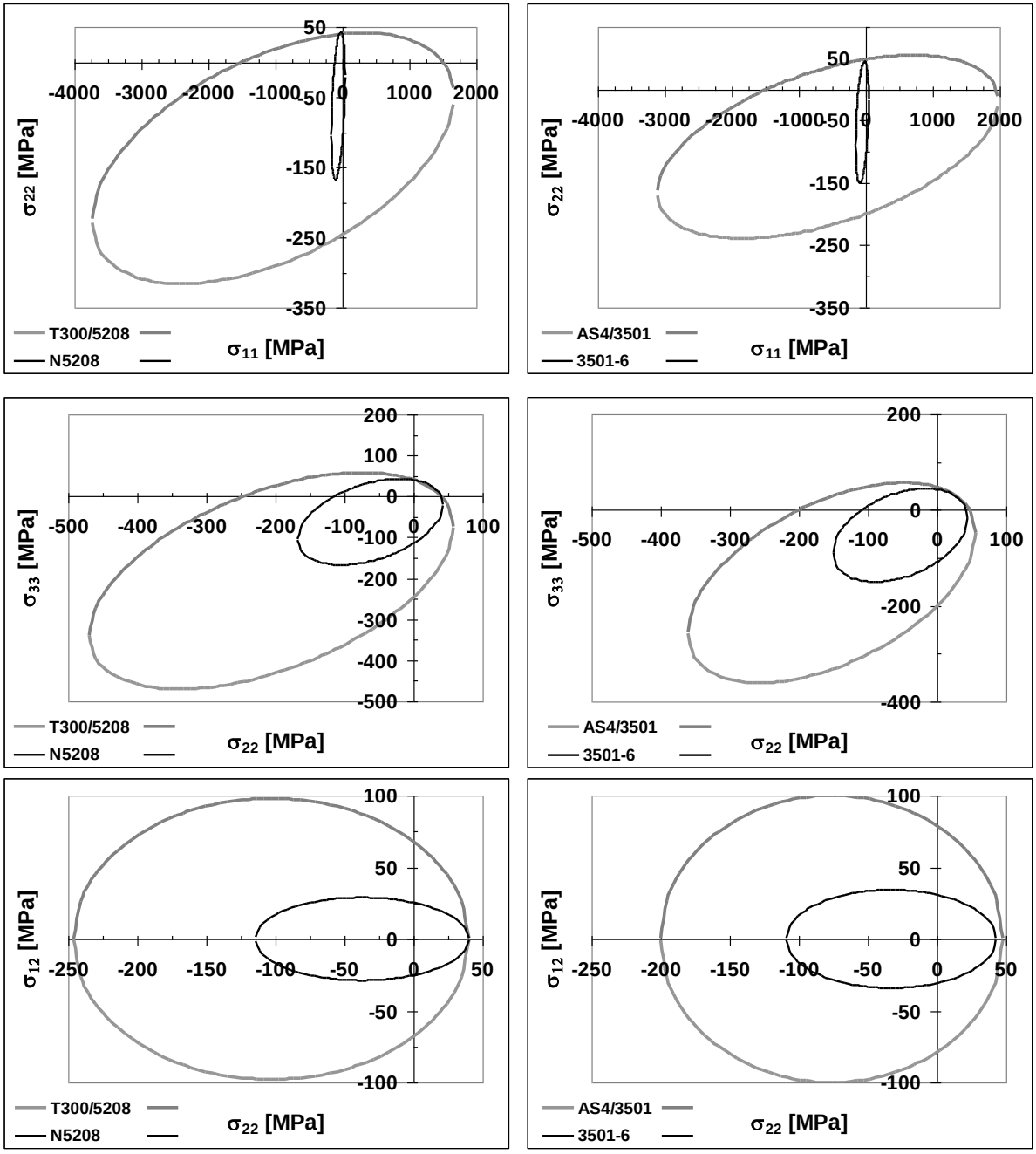

Figure 5: Examples of macroscopic and local (matrix only) stress failure envelopes of T300/5208 and AS4/3501-6 plies.

Tables

	ρ [g/cm^3]	Y_1 [GPa]	Y_2, Y_3 [GPa]	ν_{12} ν_{13}	G_{23} [GPa]	G_{12} [GPa]	M_{11} [10^{-6}/K]	M_{22}, M_{33} [10^{-6}/K]	β_{11}, β_{22} β_{33}
T300 fibers (Soden et al., 1998; Agbossou and Pastor, 1997)	1200	230	15	0.2	7	15	-1.5	27	0
N5208 epoxy matrix (Tsai, 1987; Agbossou and Pastor, 1997)	1867	4.5	4.5	0.4	6.4	6.4	60	60	0.6

Table 1: Hygro-thermo-mechanical properties of T300/5208 constituents.

Elastic	Y_1^I [GPa]	Y_2^I [GPa]	ν_{12}^I [1]	G_{12}^I [GPa]	G_{23}^I [GPa]

moduli	130	9.5	0.3	6.0	3.0
Stiffness tensor components	L^{I}_{11} [GPa]	L^{I}_{22} [GPa]	L^{I}_{12} [GPa]	L^{I}_{44} [GPa]	L^{I}_{55} [GPa]
	134.2	14.8	7.1	6.0	3.0

Table 2: Macroscopic elastic moduli (from the literature) and stiffness tensor components (calculated) considered for the composite ply at $\Delta C^{I} = 0$ % and T^{I} = 300 K, according to (Sai Ram and Sinha, 1991).

Elastic moduli	Y^{m}_{1} [GPa]	Y^{m}_{2} [GPa]	ν^{m}_{12} [1]	G^{m}_{12} [GPa]	G^{m}_{23} [GPa]
	5.35	5.35	0.350	1.98	1.98

Stiffness tensor components	L_{11}^{m} [GPa]	L_{22}^{m} [GPa]	L_{12}^{m} [GPa]	L_{44}^{m} [GPa]	L_{55}^{m} [GPa]
	8.62	8.62	4.66	1.98	1.98

Table 3: Pseudomacroscopic elastic moduli and stiffness tensor components assumed for the epoxy matrix of the composite plies at $\Delta C^{I} = 0\,\%$ and T^{I} = 300 K, according to (Herakovich, 1998).

Elastic moduli	Y_1^r [GPa]	Y_2^r [GPa]	ν_{12}^r [1]	G_{23}^r [GPa]	G_{12}^r [GPa]
Mori-Tanaka estimate	213.1	13.7	0.27	4.1	22.7

Eshelby-Kröner model	213.2	13.3	0.27	4.0	12.1
Typical expected properties	232	15	0.279	5.0	15
Stiffness tensor components	L^r_{11} [GPa]	L^r_{22} [GPa]	L^r_{12} [GPa]	L^r_{44} [GPa]	L^r_{55} [GPa]
Mori-Tanaka estimate	219.2	24.9	11.2	4.1	22.7
Eshelby-Kröner model	219.2	23.9	10.8	4.0	12.1
Typical expected properties	236.7	20.1	8.4	5.02	15

Table 4: Pseudomacroscopic elastic moduli and stiffness tensor components identified for the carbon fiber reinforcing the composite plies at $\Delta C^I = 0$ % and T^I = 300 K, according to either Mori-Tanaka estimates, or Eshelby-Kröner self-consistent model. Comparison with the corresponding properties exhibited in practice by typical high-strength carbon fibers, according to (Herakovich, 1998).

E_1 [GPa] E_2, E_3 [GPa] ν_{12}, ν_{13} ν_{23} G_{12} [GPa]

AS4 fibers (Soden et al., 1998)	225	15	0.2	0.40	15
3501-6 epoxy matrix (Soden et al., 1998)	4.2	4.2	0.34	0.34	1.567
AS4/3501-6 (KESC homogenisation)	135.2	9.2	0.25	0.36	5.2

Table 5: Macroscopic and pseudo-macroscopic mechanical elastic properties of AS4/3501-6 constituents.

Moisture expansion coefficient	β_{11}	β_{22}, β_{33}
AS4/3501-6 (Daniel and Ishai, 1994)	0.01	0.2
3501-6 epoxy from Eshelby-Kröner self-consistent inverse model	0.148	0.148
3501-6 epoxy from Mori-Tanaka inverse model	0.148	0.148

Table 6: Macroscopic and pseudomacroscopic (3501-6 matrix only) coefficients of moisture expansion of AS4/3501-6 composite. The pseudomacroscopic values results from the two inverse scale transition models described in the present work.

Applied macroscopic load	$\boldsymbol{\sigma}^{\mathbf{I}}_{\mathbf{a}} = \begin{bmatrix} 0 & 0 & 0 \\ 0 & Y^{I} & 0 \\ 0 & 0 & 0 \end{bmatrix}$, $\boldsymbol{\sigma}^{\mathbf{I}}_{\mathbf{b}} = \begin{bmatrix} 0 & 0 & 0 \\ 0 & Y^{I'} & 0 \\ 0 & 0 & 0 \end{bmatrix}$	$\boldsymbol{\sigma}^{\mathbf{I}}_{\mathbf{c}} = \begin{bmatrix} 0 & 0 & 0 \\ 0 & \sigma^{I}_{22c} & 0 \\ 0 & 0 & \sigma^{I}_{33c} \end{bmatrix}$, $\begin{cases} F^{I}_{2222}\left(\sigma^{I2}_{22c} + \sigma^{I2}_{33c}\right) + \\ 2\,F^{I}_{2233}\sigma^{I}_{22c}\sigma^{I}_{33c} + F^{I}_{22}\left(\sigma^{I2}_{22c} + \sigma^{I2}_{33c}\right) - 1 = 0 \end{cases}$	$\boldsymbol{\sigma}^{\mathbf{I}}_{\mathbf{d}} = \begin{bmatrix} 0 & S^{I} & 0 \\ S^{I} & 0 & 0 \\ 0 & 0 & 0 \end{bmatrix}$
Corresponding macroscopic strain	$\boldsymbol{\varepsilon}^{\mathbf{I}}_{\mathbf{i}} = \begin{bmatrix} \varepsilon^{I}_{11i} & 0 & 0 \\ 0 & \varepsilon^{I}_{22i} & 0 \\ 0 & 0 & \varepsilon^{I}_{33i} \end{bmatrix}$ $i = a, b$ $\quad \varepsilon^{I}_{11i} = S^{I}_{12}\sigma^{I}_{22i}$, $\varepsilon^{I}_{22i} = S^{I}_{22}\sigma^{I}_{22i}$, $\varepsilon^{I}_{33i} = S^{I}_{23}\sigma^{I}_{22i}$	$\boldsymbol{\varepsilon}^{\mathbf{I}}_{\mathbf{c}} = \begin{bmatrix} \varepsilon^{I}_{11c} & 0 & 0 \\ 0 & \varepsilon^{I}_{22c} & 0 \\ 0 & 0 & \varepsilon^{I}_{33c} \end{bmatrix}$ $\varepsilon^{I}_{11c} = S^{I}_{12}\left(\sigma^{I}_{22c} + \sigma^{I}_{33c}\right)$, $\varepsilon^{I}_{22c} = S^{I}_{22}\sigma^{I}_{22c} + S^{I}_{23}\sigma^{I}_{33c}$, $\varepsilon^{I}_{33c} = S^{I}_{23}\sigma^{I}_{22c} + S^{I}_{22}\sigma^{I}_{33c}$	$\boldsymbol{\varepsilon}^{\mathbf{I}}_{\mathbf{d}} = \begin{bmatrix} 0 & \varepsilon^{I}_{12d} & 0 \\ \varepsilon^{I}_{12d} & 0 & 0 \\ 0 & 0 & 0 \end{bmatrix}$ $\varepsilon^{I}_{12d} = S^{I}_{66}S^{I}$
Corresponding microscopic stress according to (15-17)	$\boldsymbol{\sigma}^{\mathbf{m}}_{\mathbf{i}} = \begin{bmatrix} \sigma^{m}_{11i} & 0 & 0 \\ 0 & \sigma^{m}_{22i} & 0 \\ 0 & 0 & \sigma^{m}_{33i} \end{bmatrix}$ $i = a, b, c$ (59)		$\boldsymbol{\sigma}^{\mathbf{m}}_{\mathbf{d}} = \begin{bmatrix} 0 & S^{m} & 0 \\ S^{m} & 0 & 0 \\ 0 & 0 & 0 \end{bmatrix}$
Corresponding conditions for finding the microscopic strength coefficients in stress space from (10, 19)	$\begin{cases} F^{m}_{1111}A_i + F^{m}_{1122}B_i + F^{m}_{11}C_i - 1 = 0 \\ A_i = \sigma^{m2}_{11i} + \sigma^{m2}_{22i} + \sigma^{m2}_{33i} \\ B_i = 2\left[\sigma^{m}_{11i}\left(\sigma^{m}_{22i} + \sigma^{m}_{33i}\right) + \sigma^{m}_{22i}\sigma^{m}_{33i}\right] \\ C_i = \sigma^{m}_{11i} + \sigma^{m}_{22i} + \sigma^{m}_{33i} \end{cases}$ $i = a, b, c$ (60)		$2\,F^{m}_{1212}\,S^{m2} - 1 = 0$ (61)

Table 7: one possible set of trials enabling the determination of the microscopic strength coefficients of the matrix expressed in stress space.

Strengths [MPa]	X^I	$X^{I'}$	Y^I, Z^I	$Y^{I'}$, $Z^{I'}$	S^I
T300/5208 (Tsai, 1987)	1500	1500	40	246	68
AS4/3501-6 (Liu and Tsai, 1998)	1950	1480	48	200	79

Table 8: macroscopic strength data.

Strength parameters	F^I_{1111}	F^I_{2222}, F^I_{3333}	F^I_{1212}	F^I_{1122}, F^I_{1133}	F^I_{2233}	F^I_{11}	F^I_{22}, F^I_{33}
T300/5208	$4.44\ 10^{-7}$	$1.02\ 10^{-4}$	$1.08\ 10^{-4}$	$-3.36\ 10^{-6}$	$-5.08\ 10^{-5}$	0	0.0209
AS4/3501-6	$3.46\ 10^{-7}$	$1.04\ 10^{-4}$	$8.01\ 10^{-5}$	$-3.00\ 10^{-6}$	$-5.02\ 10^{-5}$	-0.0002	0.0158

Table 9: quadratic macroscopic stress failure criteria deduced from the strength data. Quadratic *ijkl* subscripted coefficients [MPa^{-2}] and linear *ij* subscripted coefficients [MPa^{-1}].

Stiffness components	L^I_{11}	L^I_{22}, L^I_{33}	L^I_{12}, L^I_{13}	L^I_{23}	L^I_{44}	L^I_{55}, L^I_{66}
T300/5208	142.72	13.92	5.79	7.19	3.34	7.00
AS4/3501-6	137.27	11.60	4.20	5.22	3.68	6.45

Table 10: macroscopic stiffness components [GPa] of 60% volume uni-directionally fiber reinforced plies. Fiber axis is parallel to longitudinal direction.

Strength parameters	F^m_{1111}, F^m_{2222}, F^m_{3333}	F^m_{1212}	F^m_{1122}, F^m_{1133}, F^m_{2233}	F^m_{11}, F^m_{22}, F^m_{33}
N5208	$2.18\ 10^{-4}$	$7.82\ 10^{-4}$	$-8.77\ 10^{-5}$	0.0162
3501-6	$2.15\ 10^{-4}$	$5.04\ 10^{-4}$	$-8.07\ 10^{-5}$	0.0143

Table 11: quadratic local stress failure criteria in N5208 and 3501-6 epoxy matrices respectively deduced from the macroscopic failure envelopes of T300/5208 and AS4/3501-6 plies, taking into account the microscopic elastic properties given on tables 1 and 5. Quadratic *ijkl* subscripted coefficients [MPa^{-2}] and linear *ij* subscripted coefficients [MPa^{-1}].

Strengths [MPa]	X^m, Y^m, Z^m	$X^{m'}$, $Y^{m'}$, $Z^{m'}$	S^m
N5208	40.1	114.7	25.3
3501-6	42.6	108.9	30.9

Table 12: local (matrix embedded in a composite ply) strength data deduced from the local quadratic stress failure criteria of a N5208 and 3501-6 epoxy matrices respectively.